Research Paper

PAIN 166 (2025) 1296–1313

PAIN

OPEN

Activation of TGR5 in the injured nerve site according to a prevention protocol mitigates partial sciatic nerve ligation–induced neuropathic pain by alleviating neuroinflammation

Wen-Ge Shi[a,b], Yao Yao[d], Ya-Jing Liang[d], Jie Lei[a,b], Shi-Yang Feng[a,b], Zi-Xian Zhang[c], Yue Tian[c], Jie Cai[c], Guo-Gang Xing[c], Kai-Yuan Fu[a,b,*]

Abstract

Neuropathic pain is a pervasive medical challenge currently lacking effective treatment options. Molecular changes at the site of peripheral nerve injury contribute to both peripheral and central sensitization, critical components of neuropathic pain. This study explores the role of the G-protein-coupled bile acid receptor (GPBAR1 or TGR5) in the peripheral mechanisms underlying neuropathic pain induced by partial sciatic nerve ligation in male mice. TGR5 was upregulated in the injured nerve site and predominantly colocalized with macrophages. Perisciatic nerve administration of the TGR5 agonist, INT-777 according to a prevention protocol (50 μg/μL daily from postoperative day [POD] 0 to POD6) provided sustained relief from mechanical allodynia and spontaneous pain, whereas the TGR5 antagonist, SBI-115 worsened neuropathic pain. Transcriptome sequencing linked the pain relief induced by TGR5 activation to reduced neuroinflammation, which was further evidenced by a decrease in myeloid cells and pro-inflammatory mediators (eg, CCL3, CXCL9, interleukin [IL]-6, and tumor necrosis factor [TNF] α) and an increase in CD86-CD206+ anti-inflammatory macrophages at POD7. Besides, myeloid-cell-specific TGR5 knockdown in the injured nerve site exacerbated both neuropathic pain and neuroinflammation, which was substantiated by bulk RNA-sequencing and upregulated expression levels of inflammatory mediators (including CCL3, CCL2, IL-6, TNF α, and IL-1β) and the increased number of monocytes/macrophages at POD7. Furthermore, the activation of microglia in the spinal cord on POD7 and POD14 was altered when TGR5 in the sciatic nerve was manipulated. Collectively, TGR5 activation in the injured nerve site mitigates neuropathic pain by reducing neuroinflammation, while TGR5 knockdown in myeloid cells worsens pain by enhancing neuroinflammation.

Keywords: Neuropathic pain, Sciatic nerve, TGR5, Macrophages, Neuroinflammation, Inflammatory mediators

1. Introduction

Pain is an unpleasant sensory and emotional experience associated with actual or potential tissue damage or similar stimuli.[51] Neuropathic pain occurs when damage or disease affects the somatosensory nervous system.[54] Neuropathic pain contributes significantly to the global disease burden, affecting 6.9% to 10% of the global population.[6,53,60] The mechanisms underlying neuropathic pain are complex and vary between different states of the disease.[3] Currently, clinical treatments for neuropathic pain predominantly focus on drugs that regulate neural conduction. However, these drugs frequently have unavoidable side effects and less-than-ideal treatment efficacy.[2] Further research is warranted to identify new treatment targets based on distinct pathological mechanisms.

Neuropathic pain triggers neuroinflammation.[28] Following peripheral nerve injury, immune cells infiltrate the injury site, secrete cytokines and chemokines, activate local immune cells, and attract more circulating leukocytes both to the injury site and along the neural pain pathway.[18,43,59] In the peripheral nervous system, macrophages participate in pain modulation by directly

Sponsorships or competing interests that may be relevant to content are disclosed at the end of this article.

K.-Y. Fu and G.-G. Xing contributed equally to this work.

[a] Center for TMD and Orofacial Pain, Peking University School and Hospital of Stomatology, Beijing, China, [b] National Center for Stomatology & National Clinical Research Center for Oral Diseases, Beijing, China, [c] Neuroscience Research Institute, Peking University, Department of Neurobiology, School of Basic Medical Sciences, Peking University Health Science Center, Key Laboratory for Neuroscience, Ministry of Education of China & National Health, Beijing, China, [d] Department of General Dentistry and Integrated Emergency Dental Care, Beijing Stomatological Hospital, Capital Medical University, Beijing, China

**Corresponding author. Address: Center for Temporomandibular Disorders and Orofacial Pain, Peking University School and Hospital of Stomatology, No. 22, Zhongguancun South Ave, Haidian District, Beijing, 100081, China. Tel./fax: +8613910905262. E-mail address: kqkyfu@bjmu.edu.cn (K.-Y. Fu).*

Supplemental digital content is available for this article. Direct URL citations appear in the printed text and are provided in the HTML and PDF versions of this article on the journal's Web site (www.painjournalonline.com).

http://dx.doi.org/10.1097/j.pain.0000000000003460

interacting with neurons[27,57] and by releasing soluble mediators that bind to receptors expressed in other cells.[16,17,45] However, clinical trial results for patients with neuropathic pain treated with neutralizing antibodies targeting pro-inflammatory cytokines were inconclusive.[63] Therefore, a deeper understanding of the neuroimmune processes involved in the development and resolution of neuropathic pain is necessary for developing effective treatment strategies.

TGR5 is a G-protein-coupled bile acid receptor (GPBAR1) that was initially reported to mediate the anti-inflammatory effects of bile acids on lipopolysaccharide (LPS)-treated monocytes and macrophages.[32] The beneficial role of TGR5 activation in attenuating inflammation, including neuroinflammation induced by subarachnoid hemorrhage,[24,75] sepsis,[30] and intracerebroventricular injection of LPS,[65,66] has been discovered in several disease models.[48] However, the role of TGR5 in pain modulation is not well understood, and previous studies have yielded contradictory findings. On the one hand, the activation of TGR5 in sensory nerves, achieved through intraplantar or intrathecal injection of bile acids, leads to antinociception in response to mechanical paw stimulation.[1] On the other hand, TGR5 activation has been shown to promote visceral hypersensitivity in a mouse model of irritable bowel syndrome.[8]

Therefore, the aim of this study was to investigate the role of TGR5 in the peripheral mechanisms of neuropathic pain induced by partial sciatic nerve ligation (pSNL) in a mouse model.

2. Methods

2.1. Animals

Experiments were performed following the ethical principles outlined by the Animal Care and Use Committee of the Peking University Center of Health Science. Inbred 6- to 8-week-old male C57BL/6J (Vital River Laboratory Animal Technology Co Ltd, Beijing, China) and Lyz2-Cre (Cat. No. NM-KI-215037; Shanghai Model Organisms Center, Inc, Shanghai, China) mice were housed in a pathogen-free environment with a 12:12-hour light/dark cycle, an ambient temperature of 24°C ± 1°C, and an air humidity of 50% to 60%. The mice were given access to water and food ad libitum. An abundant supply of nesting materials and wooden sticks was provided in the home cage and changed every 3 days to ensure an enriched environment.

2.2. Neuropathic pain model

Neuropathic pain was induced in the mice using the pSNL model, following previously published methods with some modifications.[41,55,71] In brief, under 1% sodium pentobarbital anaesthesia, the right sciatic nerve was exposed and carefully separated from the adjacent connective tissues near the trochanter. A 9-0 silk suture with a 3/8 curved mini-needle was used to ligate approximately half of the dorsal portion of the sciatic nerve. Mice were maintained at a temperature of 37.5°C using a heated plate during operation and recovery. The anesthetic status of the mice was monitored by observing the respiration rate and checking the withdrawal reflex.

2.3. Behavioral tests

All tests were conducted during the light (rest) phase. The mice were habituated to the testing environment 2 days before testing. The investigator was blinded to the genotype and treatment of the mouse groups. Mechanical allodynia was measured using a modified version of a previously reported Von Frey test.[7,14] Von Frey filaments (Stoelting) were applied to the paw, beginning with the 0.16 g size. The presence or absence of a positive withdrawal response (flicking, licking, or lifting) determined the choice of lower- or higher-weight filaments. Four additional responses were observed after the initial change. The 50% paw withdrawal threshold was calculated based on the recorded test results.[10,15] Spontaneous pain in mice was analyzed by determining the time spent showing nocifensive behaviors (including lifting, flapping, shaking, licking, and guarding) during a 10-minute period based on video recordings.[46]

2.4. Western blotting

Under 1% sodium pentobarbital anaesthesia, the mice underwent transcardial perfusion with chilled phosphate-buffered saline (PBS). Approximately 1.5 cm of sciatic nerve tissue (including the injured site and the proximal and distal parts) was dissected distal to the semitendinosus nerve branch. Proteins in the tissues were extracted using RIPA buffer (Applygen) and 1 mM phenylmethylsulfonyl fluoride and phosphatase inhibitors were added. Proteins were separated by sodium dodecyl sulfate-polyacrylamide gel electrophoresis and transferred to the polyvinylidene difluoride membranes. The membranes were blocked using 5% nonfat milk. Subsequently, they were incubated overnight at 4°C with the following primary antibodies: rabbit anti-TGR5 (1:1000; ab72608; Abcam, Cambridge, United Kingdom), mouse anti-NLRP3 (1:1000; AG-20B-0014; AdipoGen, San Diego, CA), rabbit anti-ASC (1:1000; 67824S; Cell Signalling Technology, Danvers, MA), rabbit anti-Caspase-1 (1:1000; 24232S; Cell Signalling Technology), rabbit anti-interleukin (IL)-1β (1:200; ab9722; Abcam), mouse anti-β-Actin (1:1000; TA-09; ZSGB-BIO, Beijing, China), and rabbit anti-GAPDH (1:2000; 2118S; Cell Signalling Technology). The membranes were washed and incubated with HRP-conjugated secondary antibodies (1:1000; Immunoway, Plano, TX), and enhanced chemiluminescence detection (Tanon, St Andrews, United Kingdom) was used to visualize the proteins. Band intensities were quantified using ImageJ, and internal controls were used to calculate the relative protein expression.

2.5. Immunofluorescence staining

Under 1% sodium pentobarbital anaesthesia, the mice underwent transcardial perfusion with prewarmed 0.9% saline solution, followed by a chilled 4% paraformaldehyde solution. The spinal cord and ipsilateral sciatic nerve were dissected, fixed for 24 hours, and subsequently subjected to overnight cryoprotection at 4°C in 30% sucrose. After embedding in an Optimum Cutting Temperature Compound (Sakura), the nerve was sliced into 10 μm and the spinal cord was sliced into 30 μm thick frozen sections and affixed to slides. The sections were blocked with 10% donkey serum in PBS enriched with 0.3% Triton X-100 and incubated overnight at 4°C with the following primary antibodies: rabbit anti-TGR5 (1:500; ab72608; Abcam), mouse anti-PGP9.5 (1:1000, NB600-1160; Novus, St. Louis, MO), rat anti-mouse F4/80 (1:500; MCA497; Biorad, Hercules, CA), mouse anti-NLRP3 (1:500; AG-20B-0014; AdipoGen), rabbit anti-ASC (1:500; 67824S; Cell Signalling Technology), rabbit anti-IL-1β (1:200; ab133357; Abcam), and rabbit anti-Iba-1 (1:1000; 019-19741; WAKO) antibodies. Subsequently, appropriate secondary antibodies (1:1000; Jackson ImmunoResearch, West Grove, PA) including Cy3 donkey anti-rabbit immunoglobulin G (IgG), AF488 donkey anti-rat IgG, AF488 donkey anti-mouse IgG, Cy3 donkey anti-mouse IgG, and AF647 donkey anti-rabbit IgG were used for

incubation. Nuclear labelling was performed by counterstaining with 4′,6-diamidino-2-phenylindole.

Images were acquired using an Olympus microscope. To ensure reproducibility, a minimum of 3 sections per sample were examined. Quantitative analyses were performed blindly using ImageJ Pro Plus software (Media Cybernetics Inc).

2.6. Flow cytometry assay

Sciatic nerve cells were isolated according to a previously described protocol.[39] Approximately 1.5 cm of the sciatic nerve was carefully dissected and transferred to 200 μL of papain solution (1× HBSS [Gibco, Waltham, MA]/15 U/mL papain [Roche, Indianapolis, IN]/10 μg/mL DNase [Sigma, Burlington, MA]) on ice. After finely chopping the tissue samples into small pieces and digesting them at 37°C for 30 minutes, 400 μL of Solution A (1× HBSS/10% FBS [Gibco]/10 μg/mL DNase) was added to terminate the digestion, followed by homogenization using a 1 mL syringe fitted sequentially with a 21 and 23 G needle. After homogenization, the solution was centrifuged at 12,000 rpm for 10 seconds. The cell pellets were washed with 1 mL of FACS buffer (1× HBSS/10% FBS) and resuspended in 100 μL of FACS buffer, to which 1 μL of rat anti-mouse CD16/CD32 clone 2.4G2 (BioLegend, San Diego, CA) was added. Following 30-minute incubation on ice, the following fluorescent antibodies were added into the incubation buffer and incubated on ice for another 30 minutes: PerCP-Cy5.5 rat anti-CD11b (550993; BD Biosciences, Franklin Lakes, NJ), PE/Cyanine7 anti-mouse F4/80 (123114; BioLegend), PE anti-mouse CD86 (12-0862-81; Thermo Fisher Scientific), and APC anti-mouse CD206 (141708; BioLegend) antibodies. Subsequently, the cells were washed and resuspended in FACS buffer for flow cytometry. Cellular events were acquired using a Beckman Galios machine, and the data were analyzed using FlowJo software.

2.7. Bulk RNA-sequencing and data analysis

Total RNA was extracted from the sciatic nerve using TRIzol reagent (Life Technologies, Carlsbad, CA) and assessed for quality, concentration, and chemical purity using spectrophotometry (NanoDrop, Wilmington, DE). High-quality RNA libraries were generated and sequenced using the BGI system (Shenzhen, China). Subsequently, the sequencing data were analyzed using the Dr. Tom Multi-omics Data Mining System (available at https://biosys.bgi.com), with significance levels adjusted using a stringent threshold (Q value ≤ 0.05).

2.8. Real-time quantitative PCR analysis

Overall, 400 ng of RNA extracted from the sciatic nerve or bone marrow-derived macrophages (BMDMs) was reverse-transcribed. Subsequently, 1 μL of the resulting template complementary DNA was amplified in a 20 μL reaction volume, with 0.5 μM of the specified PCR primer. Quantitative real-time PCR was performed using an ABI 7500 Fast Real-Time PCR System (Applied Biosystems, Foster City, CA) with SYBR Premix Ex Taq II (Takara, Kusatsu, Japan) following a previously described method.[37] Specific primers were employed for amplification, including *Tgr5* (forward: 5′-ACTGGTCCTGCCTCCTTC TCC-3′, reverse: 5′-ACACTGCCATGTAGCGTTCCC-3′), *Ccl3* (forward: 5′-TTGCTGTTCTTCTCTGTACCAT-3′, reverse: 5′-AATAGTCAACGATGAATTGGCG-3′), *Ccl4* (forward: 5′-CTT GCTCGTGGCTGCCTTC-3′, reverse: 5′-TGCTGGTCTCATAGT AATCCATCAC-3′), *Tnfa* (forward: 5′-GCCTCTTCTCATTCCTGC TTGTGG-3′, reverse: 5′-GTGGTTTGTGAGTGTGAGGGTCTG-3′), *Il1b* (forward: 5′-TCGCAGCAGCACATCAACAAGAG-3′, reverse: 5′-AGGTCCACGGGAAAGACACAGG-3′), *Nlrp3* (forward: 5′-GCCGTCTACGTCTTCTTCCTTTCC-3′, reverse: 5′-CATCCG CAGCCAGTGAACAGAG-3′), and *Gapdh* (forward: 5′-AACTTT GGCATTGTGGAAGGGCTC-3′, reverse: 5′-TGGAAGAGTGGG AGTTGCTGTTGA-3′).

2.9. Cytokine measurement

Cytokines (interferon [IFN]-γ, IL-10, CCL4 [MIP-1β], IFN-α, CXCL9 [MIG], CXCL10 [IP-10], tumor necrosis factor [TNF]-α, IL-6, VEGF, IL-4, CCL3 [MIP-1α], and CCL2 [MCP-1]) in the sciatic nerve were measured using a LEGENDplex MU Cytokine Release Syndrome Panel w/FP (741023; BioLegend), following the manufacturer's protocol and analyzed using a Beckman Galios flow cytometer. Sciatic nerve tissues were homogenized in 100 μL of cold PBS. The supernatant was collected after centrifugation at 12,000*g* for 10 minutes at 4°C. Protein concentration was determined using a BCA Protein Assay Kit (Thermo Fisher Scientific). For the analysis, 25 μL of sciatic nerve extract was used. The reported values in pg/mL were normalized to pg/mg of total protein, considering the protein concentration.

2.10. Lentivirus-mediated shRNA construction

The shRNA lentivirus for knockdown sequence identification was constructed by OBiO Technology (Shanghai, China) using the lentiviral vector, pSLenti-U6-shRNA-CMV-mCherry-F2A-Puro-WPRE. The 3 sequences targeting *GPBAR1* mRNA were as follows: 5′-CCTACCTCTACCTGGAAGTTT-3′ (shGPBAR1-1), 5′-CTCTGTTATCGCTCATCTCAT-3′ (shGPBAR1-2), and 5′-TGCTTCTTCCTAAGCCTACTA-3′ (shGPBAR1-3). The sequence of the control shRNA was 5′-CCTAAGGTTAAGTCG CCCTCG-3′ (referred to as shControl). The viral titers of shGPBAR1 and shControl reached 2.7×10^8 and 7.7×10^8 TU/mL, respectively.

A Cre-dependent shRNA lentivirus for TGR5-specific knockdown was constructed by BrainVTA (Wuhan, China). The lentiviral vector sequence was rLV-CMV-DIO-EGFP-5′miR30-shRNA-3′miR30-WPRE. The sequence targeting *GPBAR1* mRNA was 5′-CCTACCTCTACCTGGAAGTTT-3 and named shGPBAR1. The viral titers of shGPBAR1 and shControl reached 1×10^9 TU/mL.

2.11. Bone marrow-derived macrophage culture and treatments

The isolation and incubation of BMDMs were performed following a well-established protocol with minor adjustments.[49] In brief, cells in the femur and tibia were flushed out of the bone using sterile HBSS. Following filtration through a 70-μm cell strainer, the cell solution was lysed using a lysis buffer (Solarbio) to remove the blood cells. After centrifugation, the cell pellets were suspended in 10 mL of complete medium (RPMI 1640 medium [Gibco]/5 mM penicillin/streptomycin [Gibco]/10% FBS/30 ng/mL macrophage colony-stimulating factor [BioLegend]) and plated in a 10-cm dish for incubation at 37°C in a 5% CO_2 atmosphere.

For lentivirus transfection, BMDMs incubated for 3 days were infected with fresh complete medium containing lentiviruses at a multiplicity of infection of 100 for 12 hours. After discarding the lentiviruses, the cells were cultured for an additional 72 to 96 hours in a fresh complete medium and then prepared for

Western blotting, immunofluorescence staining, and real-time quantitative PCR (RT-qPCR) analysis.

2.12. Perisciatic nerve injection

Perineural injections were administered according to a previously established protocol.[34] In brief, a 30-gauge needle attached to a micro-syringe was gently inserted into the scar site induced by the pSNL procedure. The substances were administered to the region surrounding the sciatic nerve in the upper thigh of the hind limb. Successful injection and targeting of the sciatic nerve were confirmed using fast green dye, which was deposited in the nerve after injection.

The TGR5-specific agonist, INT-777 (HY-15677; MedChemExpress, Monmouth Junction, NJ), was dissolved in 10% dimethylsulfoxide (DMSO) to the concentrations of 0.5 μg/μL, 5 μg/μL, and 50 μg/μL. The TGR5-specific antagonist, SBI-115 (HY-111534; MedChemExpress), was dissolved in 10% DMSO to a concentration of 40 μg/μL. A 4 μL volume of INT-777, SBI-115, or 10% DMSO was administered daily through perisciatic nerve injection following a prevention protocol that started during surgery and continued until 6 days postsurgery day. All injections were made under isoflurane anesthesia.

Cre-dependent shRNA lentivirus (shGPBAR1 or shControl) was perineurally injected at a final titer of 1×10^9 TU/mL in a total volume of 4 μL per mouse following a prevention protocol applied concurrently with pSNL surgery. Additional injections were administered on the first and second days following pSNL surgery under isoflurane anesthesia.

2.13. Data analysis

Statistical analyses were performed using GraphPad Prism software version 9.0. Data are presented as mean ± SEM. The mean values of the 2 groups were compared using the 2-tailed unpaired Student *t* test. Data from multiple groups were compared using 1-way analysis of variance (ANOVA), followed by Tukey post hoc test. The *F*-statistics for 1-way ANOVA were reported as *F*(*df* of treatment, residual). Two-factor interaction analyses were conducted using 2-way ANOVA with Šídák post hoc test, and *F*-statistics were reported as *F*(*df* of interaction, treatment, time/residual). Significance levels were denoted as follows: $^*P < 0.05$, $^{**}P < 0.01$, and $^{***}P < 0.001$.

3. Results

3.1. TGR5 increased in the sciatic nerve after partial sciatic nerve ligation and was mainly colocalized with macrophages

Partial sciatic nerve ligation–induced mechanical allodynia indicated by a decreased paw withdrawal threshold in the mouse model of neuropathic pain was detected on postoperative day (POD) 1 and persisted until POD14 ($F(4, 55) = 3.785$, $F(4, 55) = 10.99$, $F(1, 55) = 70.82$) (**Fig. 1A**). TGR5 expression in the injured sciatic nerve was determined using Western blotting (**Fig. 1B**). The results indicated that the protein levels of TGR5 significantly and continuously increased starting on POD1, peaked at POD7, and remained elevated until POD14 ($F(4, 15) = 21.13$) (**Fig. 1C**).

To investigate the cellular localization of TGR5, double-staining for TGR5 and F4/80 (a macrophage marker) was performed on the sciatic nerve in both sham and pSNL groups (**Fig. 1D**). Consistent with our Western blotting data, the number of TGR5-positive cells detected by fluorescence staining significantly increased in the sciatic nerve, particularly at the site of injury (**Fig. 1E**). Notably, TGR5 predominantly colocalized with F4/80-positive cells. Quantitative analysis revealed that the colocalization ratio of TGR5 with F4/80, indicated by the percentage of area overlap, was significantly higher in the POD7 group compared with the sham group (**Fig. 1F**). Given the confirmed expression of TGR5 in neurons, we subsequently double-stained TGR5 with PGP9.5 (a nerve fiber marker) in sciatic nerves (Fig. S1A, available at http://links.lww.com/PAIN/C168). The results showed an increase in TGR5 after pSNL, with minimal PGP9.5 colocalization, and no significant differences between the sham and POD7 groups (Figs. S1B and C, available at http://links.lww.com/PAIN/C168). In addition, immunofluorescent staining indicated that some F4/80-positive macrophages were closely associated with PGP9.5-positive nerve fibers, resulting in overlapping staining of F4/80 and PGP9.5 (Fig. S1D, available at http://links.lww.com/PAIN/C168). Triple-staining micrographs of TGR5, F4/80, and PGP9.5 suggested that what appeared to be colocalization of TGR5 with PGP9.5 was actually colocalization with macrophages adjacent to nerve fibers (Fig. S1E, available at http://links.lww.com/PAIN/C168). Consequently, the colocalization ratio of TGR5 with nerve fibers in the sciatic nerve was low. Overall, these findings revealed that TGR5 expression increases in sciatic nerves after pSNL, with predominant location in macrophages.

3.2. Macrophages in the sciatic nerve underwent dynamic changes following partial sciatic nerve ligation

To confirm the involvement of macrophages in the pathological process induced by pSNL, the alterations of macrophages in the sciatic nerve were assessed using flow cytometry (Fig. S2, available at http://links.lww.com/PAIN/C168). The results indicated a significant increase in the percentage of CD11b+ myeloid cells at POD1 and POD3 ($F(4, 17) = 12.40$) (**Fig. 2A**). Compared with the sham group, the percentages of F4/80+ and CD11b+F4/80+ macrophages were significantly increased at POD3 ($F(4, 17) = 7.575$; $F(4, 17) = 7.127$) (**Figs. 2B and C**). In addition, the population of $CD86^+CD206-$ pro-inflammatory macrophages was increased at POD1, showed a relative decrease at POD3 and POD7, and eventually returned to the levels of the sham group by POD14 ($F(4, 17) = 96.77$) (**Fig. 2D**). The percentage of CD86-CD206+ anti-inflammatory macrophages followed a pattern opposite to that of $CD86^+CD206-$ macrophages ($F(4, 17) = 14.13$) (**Fig. 2E**). Consequently, the ratio of $CD86^+CD206-$ macrophages to CD86-CD206+ macrophages significantly increased at POD1 ($F(4, 17) = 9.327$) (**Fig. 2F**). Overall, macrophages were increased in the sciatic nerve after pSNL, displaying pro-inflammatory characteristics.

3.3. Perisciatic nerve injection of the TGR5 agonist alleviated partial sciatic nerve ligation–induced neuropathic pain, while administration of the TGR5 antagonist exaggerated neuropathic pain

Given the significant changes in TGR5 expression following pSNL and its predominant colocalization with macrophages, it was hypothesized that TGR5 plays a role in pSNL-induced mechanical allodynia. To test this, the TGR5 agonist INT-777 was administered daily through perisciatic nerve injection from day 0 to day 6, and pain-like behaviours were assessed (**Fig. 3A**). Among the 3 dosing regimens tested, mice treated with 50 μg/μL INT-777 showed a significant recovery in the 50% paw withdrawal threshold, while those that received 0.5 μg/μL or 5 μg/μL did not ($F(16, 125) = 1.860$, $F(4, 125) = 9.652$, $F(4, 125) = 14.94$) (Fig. S3A, available at http://links.lww.com/PAIN/C168). To

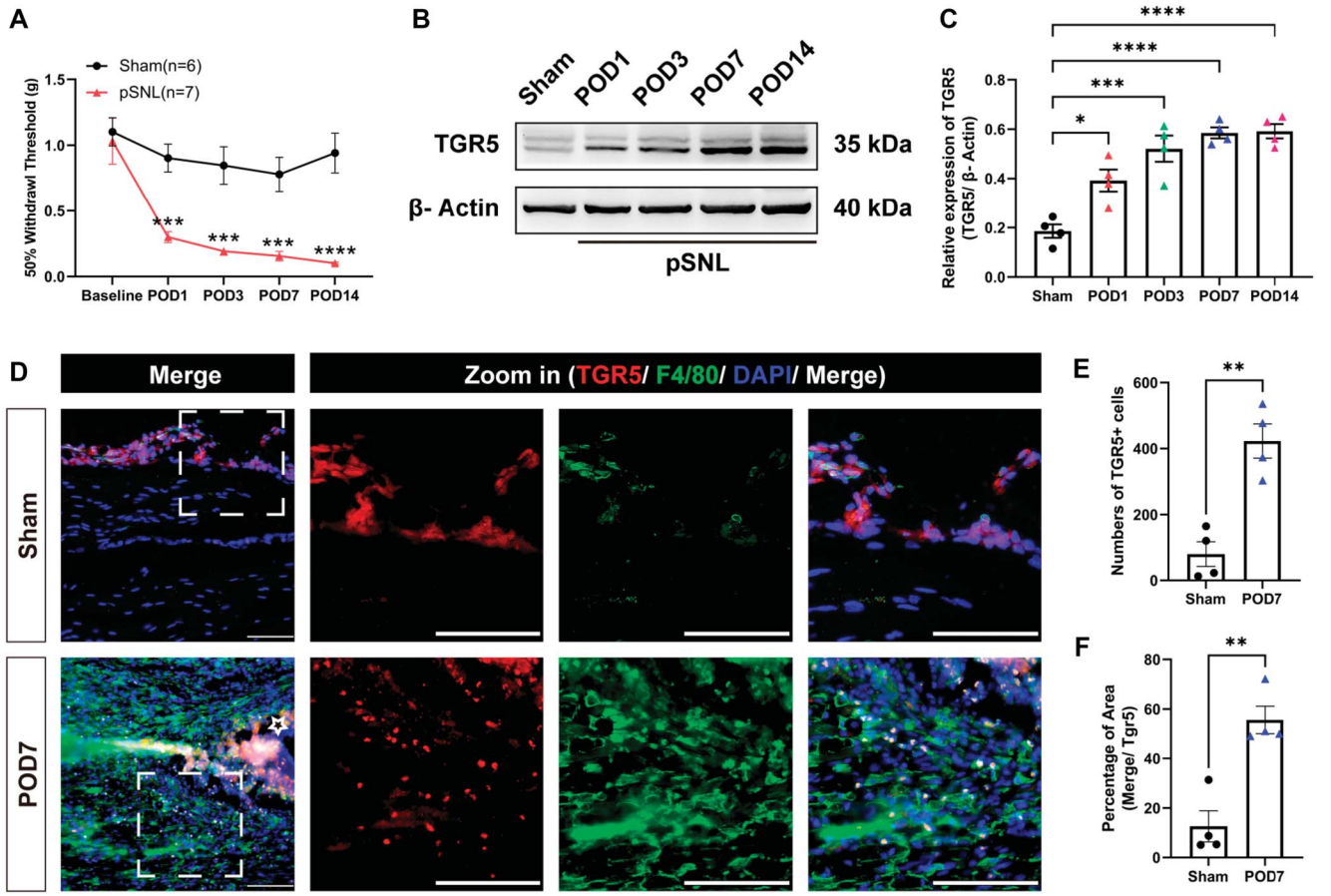

Figure 1. Expression of TGR5 in the sciatic nerve after pSNL. (A) Alterations in the 50% paw withdrawal threshold assessed through the Von Frey test after pSNL. n = 6 to 7 per group. ***$P < 0.001$, ****$P < 0.0001$ vs sham group; 2-way ANOVA, Šídák post hoc test, F (4, 55) = 3.785, F (4, 55) = 10.99, F (1, 55) = 70.82. (B) Representative Western blotting bands at different time points. (C) Densitometric quantification of TGR5 in the ipsilateral (right) sciatic nerve following pSNL. The sciatic nerves of the sham mice were collected 7 days after the sham operation. n = 4 per group. *$P < 0.05$, ***$P < 0.001$, ****$P < 0.0001$ vs sham group; 1-way ANOVA, Tukey post hoc test, F (4, 15) = 21.13. Data are presented as the mean ± SEM. (D) Representative microphotographs illustrating co-immunofluorescence staining of TGR5 (red) with macrophages (F4/80, green) in the sciatic nerve. Pentagrams indicate the site of injury. Nuclei were stained with DAPI (blue). Scale bar: 100 μm. Number of TGR5-positive cells (E) and percentage of TGR5 colocalized with macrophages in the overall TGR5-positive area (F) in the sciatic nerve. n = 3 to 4 per group. **$P < 0.01$; unpaired t test. Data are presented as the mean ± SEM. ANOVA, analysis of variance; pSNL, partial sciatic nerve ligation.

investigate the short-term effects of INT-777, behavioral tests were conducted both before the injection and 1 hour after injection. The results revealed a trend towards recovery in the 50% paw withdrawal threshold postinjection, though the changes from preinjection values were not statistically significant. The notable anti-allodynic effect of INT-777 began on POD5, before injection, likely due to the cumulative effect of multiple injections (F (14, 160) = 7.922, F (7, 160) = 26.49, F (2, 160) = 344.0) (**Fig. 3B**). This effect persisted until POD21, even after cessation of the drug administration (F (12, 168) = 3.016, F (6, 168) = 17.44, F (2, 168) = 65.53) (**Fig. 3C**). In addition, INT-777 significantly and continuously reduced spontaneous nocifensive behavior from POD5 onward (F (16, 180) = 11.85, F (8, 180) = 51.01, F (2, 180) = 491.1) (**Fig. 3D**).

To determine whether the upregulated TGR5 in the injured nerve site was activated by endogenous ligands, a perisciatic injection of the TGR5 antagonist, SBI-115 (40 μg/μL) was administered following the same protocol used for INT-777. Blocking TGR5 significantly exacerbated pain-like behaviors in mice after pSNL (F (8, 126) = 1.556, F (8, 126) = 166.2, F (1, 126) = 43.14) (F (8, 126) = 2.293, F (8, 126) = 84.64, F (1, 126) = 17.84) (**Figs. 3E and F**). In addition, sham mice treated with SBI-115 showed a reduced 50% paw withdrawal threshold and increased nocifensive behaviors at POD5 and POD7, with a return to baseline parameters by POD14. In contrast, INT-777 administration did not alter pain-like behaviors in sham mice (F (16, 153) = 2.373, F (8, 153) = 0.9100, F (2, 153) = 14.80) (F (16, 153) = 1.099, F (8, 153) = 3.087, F (2, 153) = 15.67) (Figs. S3B and C, available at http://links.lww.com/PAIN/C168). The general health status of the mice, which was assessed by body weight, remained stable throughout the experiment, unaffected by either the pSNL surgery or the perisciatic injection (F (6, 84) = 0.6498, F (2, 84) = 29.37, F (3, 84) = 0.6073) (Fig. S3D, available at http://links.lww.com/PAIN/C168). These findings suggested that upregulated TGR5 in the injured sciatic nerve is indeed activated by endogenous ligands. While this activation is beneficial, it is not sufficient alone to prevent the progression of neuropathic pain, which could be further mitigated by the exogenous ligand INT-777.

3.4. Partial sciatic nerve ligation–induced transcriptome alterations reversed by INT-777 administration were predominantly inflammation-related

To illustrate the upstream mechanisms of mechanical allodynia alleviation induced by INT-777 treatment, the transcriptional

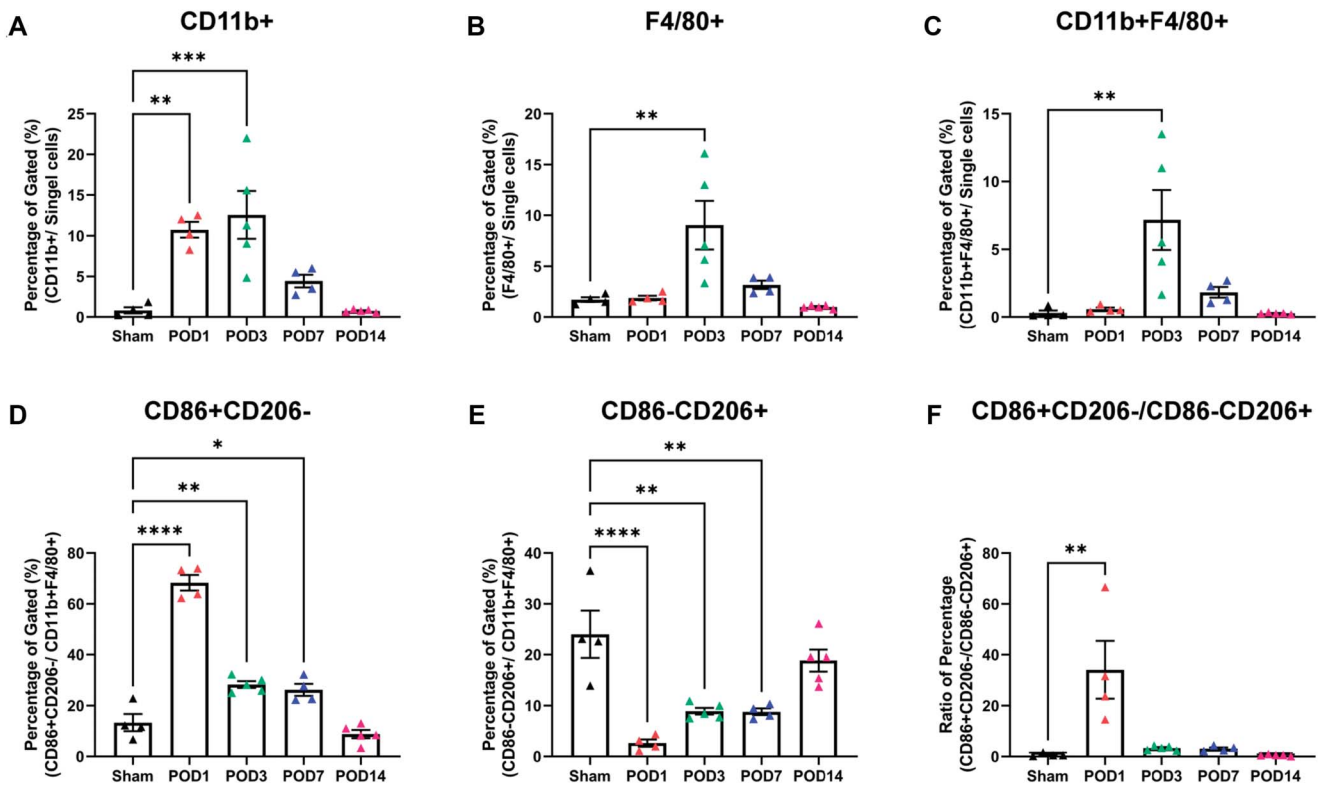

Figure 2. Alterations of macrophages in the sciatic nerve after pSNL. Percentages of CD11b+ cells (F (4, 17) = 12.40) (A), F4/80+ cells (F (4, 17) = 7.575) (B), and CD11b+F4/80+ cells (F (4, 17) = 7.127) (C) among single cells, defined by FS-A and FS-W. Percentages of $CD86^{+}CD206-$ cells (F (4, 17) = 96.77) (D) and CD86-CD206+ cells (F (4, 17) = 14.13) (E) among CD11b+F4/80+ cells. (F) The ratio of $CD86^{+}CD206-$ macrophages to CD86-CD206+ macrophages (F (4, 17) = 9.327). The sciatic nerves of the sham mice were collected 7 days after the sham operation. n = 4 to 5 per group. $^{*}P < 0.05$, $^{**}P < 0.01$, $^{***}P < 0.001$, $^{****}P < 0.0001$ vs sham group; 1-way ANOVA, Tukey post hoc test. Data are presented as the mean ± SEM. ANOVA, analysis of variance; pSNL, partial sciatic nerve ligation.

profile of the sciatic nerve from the 3 groups, DMSO_Sham, DMSO_pSNL, and INT-777_pSNL, was analyzed at POD3 using bulk RNA-sequencing (RNA-seq) (**Fig. 4A**). Principal component analysis revealed distinct transcriptome characteristics among the 3 groups (**Fig. 4B**). Specifically, 562 and 556 downregulated and upregulated genes (clusters 1 and 2 in Fig. S4A, available at http://links.lww.com/PAIN/C168), respectively, were detected in the DMSO_pSNL group when using the DMSO_Sham group for comparison (definition of differentially expressed genes [DEGs]: | log2FC | ≥ 2 and Q value ≤ 0.05; **Fig. 4C**). Compared with vehicle treatment, following INT-777 treatment 156 DEGs were downregulated and 84 DEGs were upregulated after pSNL (**Fig. 4C**, clusters 3 and 4 in Fig. S4B, available at http://links.lww.com/PAIN/C168).

To understand the functions of DEGs, the biological processes involved in 4 gene clusters were analyzed separately using Gene Ontology (GO) enrichment analysis. Specifically, DEGs in cluster 1 were mainly related to the biosynthetic and metabolic processes of sterol, steroid, and cholesterol (Fig. S4C, available at http://links.lww.com/PAIN/C168). DEGs in cluster 2 were primarily related to the inflammatory response and processes associated with cytokines and chemokines (Fig. S4D, available at http://links.lww.com/PAIN/C168). Differentially expressed genes in cluster 3 were mainly related to the immune response (Fig. S4E, available at http://links.lww.com/PAIN/C168). Differentially expressed genes in cluster 4 were majorly related to sarcomere organization, muscle contraction, and organism development (Fig. S4F, available at http://links.lww.com/PAIN/C168). Notably, DEGs in clusters 2 and 3, which were genes upregulated after pSNL and genes downregulated after INT-777 treatment, respectively, were involved in similar biological processes. Specifically, there were 29 overlapping genes between the 2 clusters (**Figs. 4D and E**). GO-enrichment analysis indicated that these genes were involved in immune system function, regulation of IL-1β and TNF production, cellular response to IFN-γ, and chemotaxis (**Fig. 4F**). Kyoto Encyclopedia of Genes and Genomes (KEGG) pathway enrichment analysis indicated that these genes were associated with cytokine and cytokine receptor interaction, toll-like receptor signaling, and NF-kappa B signaling pathways among other pathways (**Fig. 4G**).

Overall, bulk RNA-seq data indicated that the transcriptome alterations in the sciatic nerve induced by pSNL and further reversed by TGR5 activation were closely associated with the inflammatory response, particularly genes related to the production of pro-inflammatory cytokines and chemokines. The regulation of these inflammatory mediators may play a pivotal role in the mechanisms underlying the mechanical allodynia alleviation induced by INT-777 treatment.

3.5. Partial sciatic nerve ligation–induced increase of pro-inflammatory mediators and monocytes/macrophages in the sciatic nerve were partially reversed by INT-777 administration

To verify the effect of INT-777 administration on cytokine/chemokine expression, mice were killed on POD7 and the sciatic nerve was subjected to cytometric bead array analysis. The results indicated that CCL3, CXCL9, TNF-α, and IL-6 increased

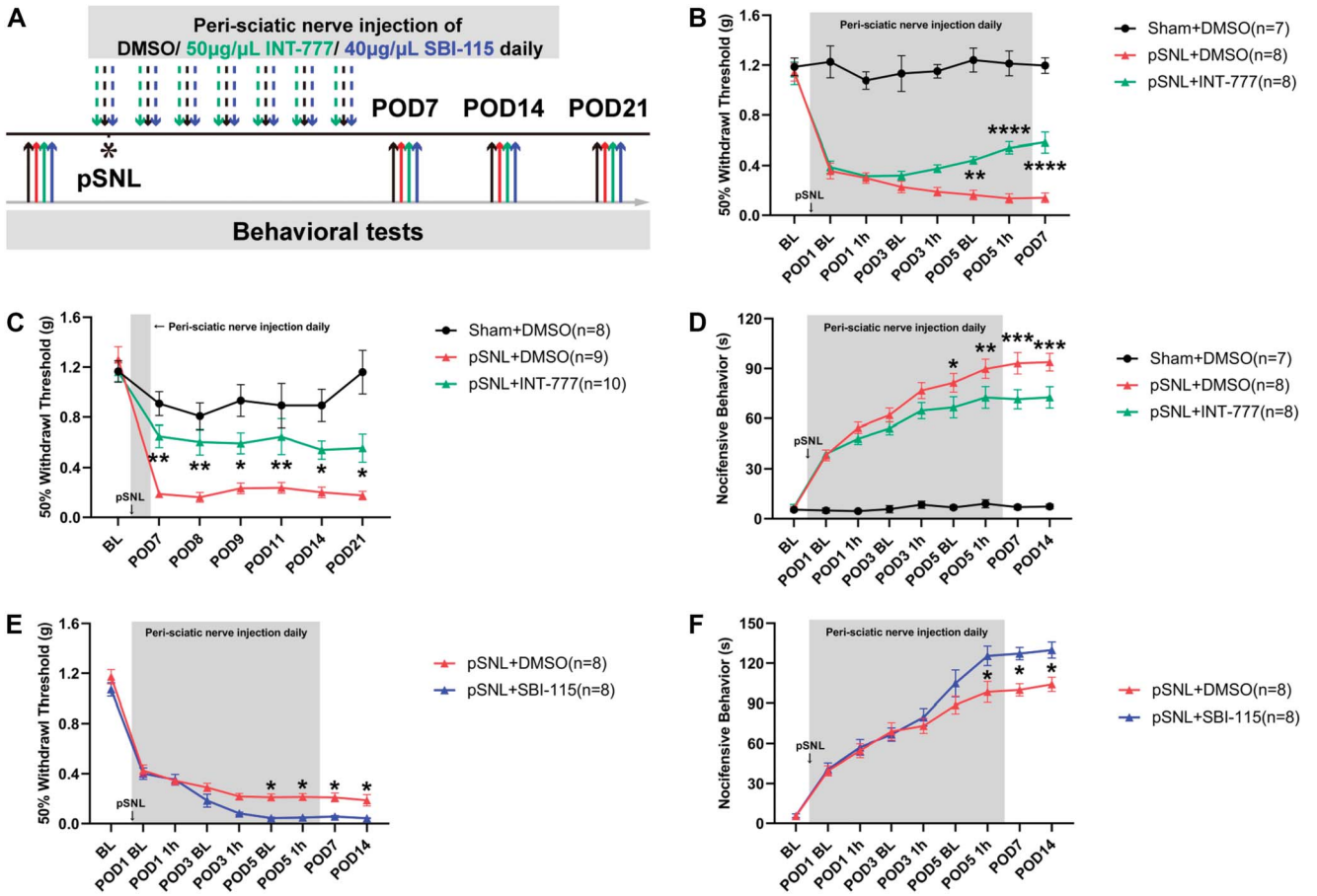

Figure 3. Effects of perisciatic nerve administration of the TGR5 agonist, INT-777 or the TGR5 antagonist, SBI-115 on pSNL-induced neuropathic pain. (A) Schematic of experimental design. (B) Alterations in the 50% paw withdrawal threshold were evaluated before injection and 1 hour after daily DMSO or INT-777 (50 μg/μL) administration following a prevention protocol. n = 7 to 8 per group. $^{**}P < 0.01$, $^{****}P < 0.0001$ vs pSNL+DMSO group; 2-way ANOVA, Šídák post hoc test, $F(14, 160) = 7.922$, $F(7, 160) = 26.49$, $F(2, 160) = 344.0$. (C) Alterations in the 50% paw withdrawal threshold were evaluated following the discontinuation of perisciatic nerve treatment. n = 8 to 10 per group. $^{*}P < 0.05$, $^{**}P < 0.01$ vs pSNL+DMSO group; 2-way ANOVA, Šídák post hoc test, $F(12, 168) = 3.016$, $F(6, 168) = 17.44$, $F(2, 168) = 65.53$. (D) Alterations in the time spent on nocifensive behaviors (including lifting, licking, flapping, and shaking) by mice before injection and 1 hour after injection during a 10-minute period were evaluated at POD1, POD3, POD5, POD7, and POD14. n = 7 to 8 per group. $^{*}P < 0.05$, $^{**}P < 0.01$, $^{***}P < 0.001$ vs pSNL+DMSO group; 2-way ANOVA, Šídák post hoc test, $F(16, 180) = 11.85$, $F(8, 180) = 51.01$, $F(2, 180) = 491.1$. (E) Alterations in the 50% paw withdrawal threshold were evaluated before injection and 1 hour after daily DMSO or SBI-115 (40 μg/μL) administration following a prevention protocol. n = 8 per group. $^{*}P < 0.05$ vs pSNL+DMSO group; 2-way ANOVA, Šídák post hoc test, $F(8, 126) = 1.556$, $F(8, 126) = 166.2$, $F(1, 126) = 43.14$. (F) Alterations in the time spent on nocifensive behaviors by mice before injection and 1 hour after daily DMSO or SBI-115 (40 μg/μL) administration according to a prevention protocol. n = 8 per group. $^{*}P < 0.05$ vs pSNL+DMSO group; 2-way ANOVA, Šídák post hoc test, $F(8, 126) = 2.293$, $F(8, 126) = 84.64$, $F(1, 126) = 17.84$. Data are presented as the mean ± SEM. ANOVA, analysis of variance; BL, baseline; DMSO, dimethylsulfoxide; POD, postoperative day; pSNL, partial sciatic nerve ligation.

in the injured nerve site after pSNL, and the administration of 50 μg/μL INT-777 prevented their upregulation (F (2, 21) = 18.27; F (2, 21) = 4.893; F (2, 21) = 8.638; F (2, 21) = 21.10) (**Figs. 5A–D**). In addition, the expression levels of CCL2, CXCL10, and VEGF, which were all altered by pSNL, remained unchanged following INT-777 treatment (F (2, 21) = 27.90; F (2, 21) = 4.403; F (2, 21) = 5.123) (Figs. S5A–D, available at http://links.lww.com/PAIN/C168). Unexpectedly, no differences were detected in the expression of CCL4, IL-4, IL-10, IFN-α, and IFN-γ among the 3 groups (F (2, 21) = 1.284; F (2, 19) = 1.306; F (2, 19) = 1.279; F (2, 21) = 0.2200; F (2, 21) = 0.3170) (Figs. S5E–H, available at http://links.lww.com/PAIN/C168).

To assess the impact of local TGR5 activation on monocytes and macrophages, the sciatic nerve from mice treated with DMSO or INT-777 for 7 days was analyzed using flow cytometry (**Fig. 5E**). The results showed a significant reduction in the percentages of CD11b+ monocytes and CD11b+F4/80+ macrophages following INT-777 treatment, although the percentage of F4/80+ cells did not significantly differ between the 2 groups (**Figs. 5F–H**). While the individual percentage of $CD86^{+}CD206-$ macrophages remained unchanged, administration of 50 μg/μL INT-777 significantly increased the percentage of CD86-CD206+ macrophages and decreased the ratio of $CD86^{+}CD206-$ to CD86-CD206+ macrophages in the treated sciatic nerve (**Figs. 5I–K**).

These results indicated that INT-777 administered according to a prevention protocol significantly decreased pro-inflammatory mediators, reduced the total number of monocyte/macrophages, and increased the prevalence of anti-inflammatory macrophages in the sciatic nerve. Collectively, these results showed that local TGR5 activation results in reduced neuroinflammation.

3.6. Myeloid-cell-specific TGR5 knockdown in the sciatic nerve exacerbated partial sciatic nerve ligation–induced neuropathic pain

Macrophages in the sciatic nerve include tissue-resident peripheral nerve and infiltrating monocyte-derived macrophages. In the physiological conditions, resident macrophages are slowly renewed from BMDMs. Upon injury, macrophages in the sciatic

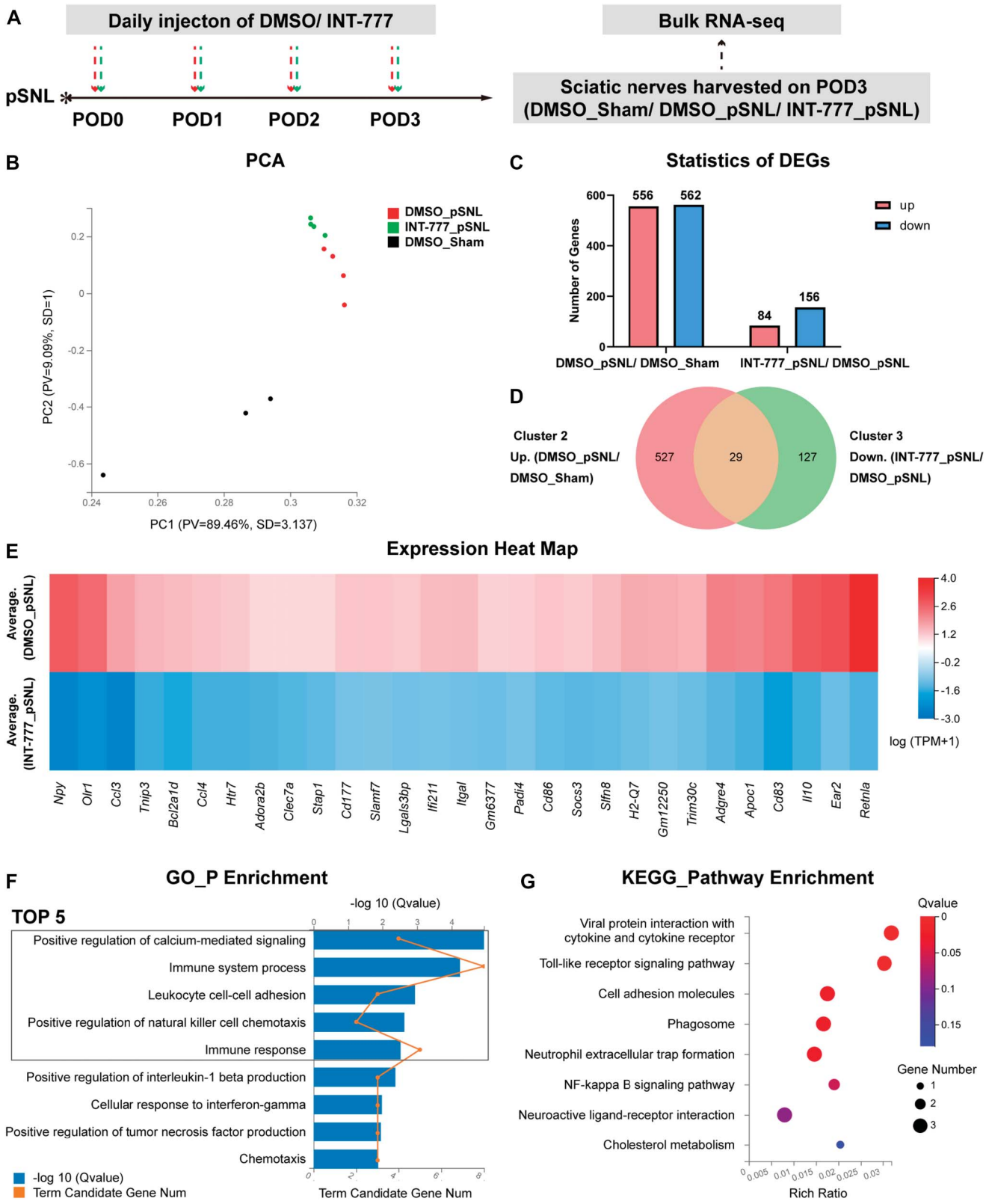

Figure 4. Transcriptome alterations in the sciatic nerve rescued by administration of INT-777 after pSNL at POD3. (A) Schematic of experimental design. (B) PCA of the sciatic nerve in the 3 groups. n = 3 to 4 per group. (C) Diagram illustrating the DEGs in the DMSO_pSNL group compared with those in the DMSO_Sham group and the DEGs in the INT-777_pSNL group compared with those in the DMSO_pSNL group. (D) Venn diagram illustrating the overlapping genes between cluster 2 (upregulated DEGs in the DMSO_pSNL group compared with those in the DMSO_Sham group) and cluster 3 (downregulated DEGs in the INT-777_pSNL group compared with those in the DMSO_pSNL group). (E) Heat map of 29 overlapping genes from the Venn diagram. (F) GO-enriched biological processes of 29 overlapping DEGs. (G) KEGG-enriched pathways of 29 overlapping DEGs. DEG, differentially expressed gene; DMSO, dimethylsulfoxide; GO, Gene Ontology; KEGG, Kyoto Encyclopedia of Genes and Genomes; PCA, principal component analysis; POD, postoperative day; pSNL, partial sciatic nerve ligation; pSNL, partial sciatic nerve ligation.

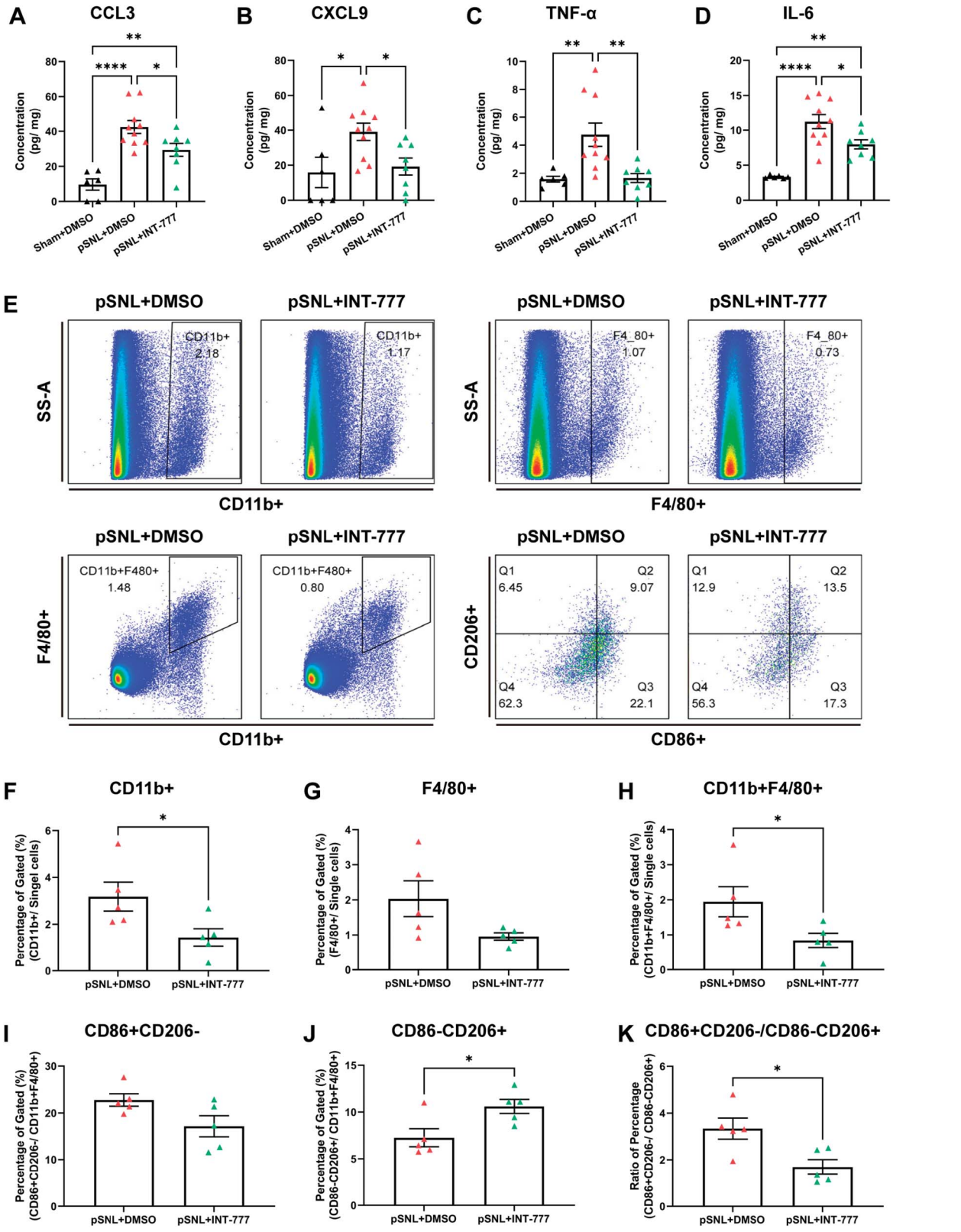

Figure 5. Effects of INT-777 administration on alterations in inflammatory mediators and macrophages induced by pSNL at POD7. Protein levels of CCL3 (F (2, 21) = 18.27) (A), CXCL9 (F (2, 21) = 4.893) (B), TNF-α (F (2, 21) = 8.638) (C), and IL-6 (F (2, 21) = 21.10) (D) in the sciatic nerve at POD7 were measured using cytometric bead array analysis. n = 4 to 5 per group. The displayed data originated from 2 independent repeated tests. $^{*}P < 0.05$, $^{**}P < 0.01$, $^{****}P < 0.0001$; 1-way ANOVA, Tukey post hoc test. (A) (E) Representative flow cytometry pseudocolor dot plots of myeloid cell populations in the sciatic nerve at POD7 in mice treated with DMSO or INT-777. Percentages of CD11b+ cells (F), F4/80+ cells (G), and CD11b+F4/80+ cells (H) among single cells, defined by FS-A and FS-W. Percentages of $CD86^{+}CD206-$ cells (I) and CD86-CD206+ cells (J) among CD11b+F4/80+ cells. (K) The ratio of $CD86^{+}CD206-$ macrophages to CD86-CD206+ macrophages. n = 5 per group. $^{*}P < 0.05$; unpaired t test. Data are presented as the mean ± SEM. ANOVA, analysis of variance; DMSO, dimethylsulfoxide; POD, postoperative day; pSNL, partial sciatic nerve ligation.

nerve have been shown to be predominantly circulating monocyte-derived macrophages.[72] To gain further insights into the contribution of macrophage-produced TGR5 in the injured sciatic nerve to pain perception, targeted knockdown of TGR5 in myeloid cells was performed in Lyz2-Cre mice with the shGPBAR1 sequence. The most effective shRNA sequence was selected from 3 different sequences depending on its ability to reduce the mRNA expression of *Tgr5* in BMDMs (Fig. S6A, available at http://links.lww.com/PAIN/C168). Finally, the sequence of shGPBAR1-1 was designated as shGPBAR1 and further used. The specific knockdown effect of the LV-CMV-DIO-EGFP-shRNA (shGPBAR1) virus was validated in BMDMs from Lyz2-Cre mice using RT-qPCR (Fig. S6B, available at http://links.lww.com/PAIN/C168), immunofluorescence staining (Figs. S6C and D, available at http://links.lww.com/PAIN/C168), and Western blotting (Figs. S6E and F, available at http://links.lww.com/PAIN/C168).

Considering that the increase of myeloid cells in the sciatic nerve was most significant during the first 3 days after pSNL, the perisciatic nerve injection of lentivirus was performed 3 times postoperatively (**Fig. 6A**). To evaluate the cell specificity of virus infection, mice were killed on POD7 and the sciatic nerve was

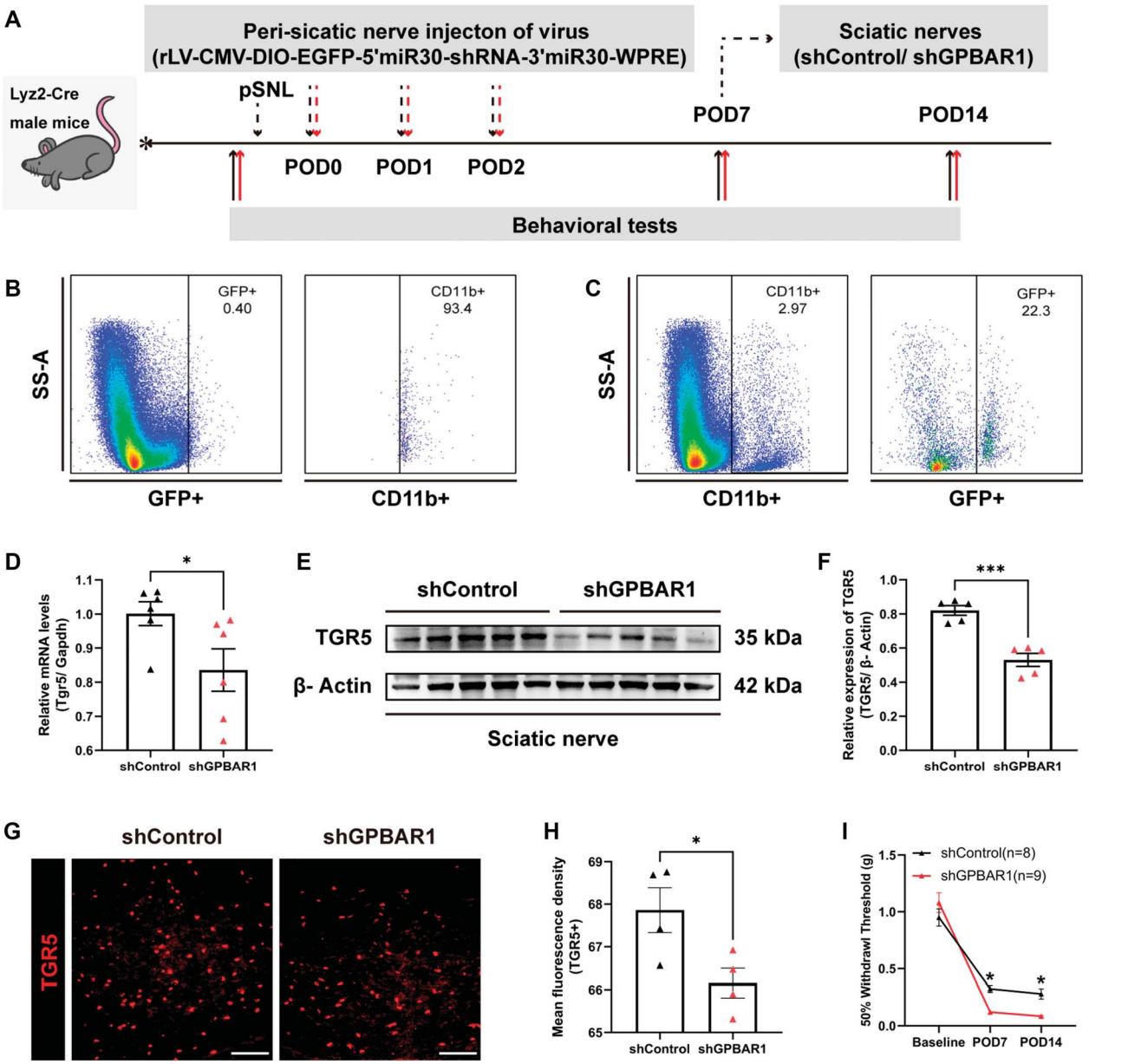

Figure 6. Validation of myeloid-cell-specific TGR5 knockdown and the effect of TGR5 knockdown on mechanical allodynia. (A) Schematic of experimental design. Representative flow cytometry pseudocolor dot plots indicating the percentage of CD11b+ cells among all GFP+ cells (B) and the percentage of GFP+ cells among all CD11b+ cells (C) in the sciatic nerve of mice 5 days after virus injection. (D) mRNA expression of *Tgr5* in the sciatic nerve of Lyz2-Cre mice treated with shControl virus or shGPBAR1 virus. n = 6 per group. $^{*}P < 0.05$; unpaired *t* test. (E) Representative Western blotting bands and (F) densitometric quantification of TGR5 in the sciatic nerve of Lyz2-Cre mice treated with shControl virus or shGPBAR1 virus after pSNL. n = 5 per group. $^{***}P < 0.001$; unpaired *t* test. (G) Representative microphotographs of immunofluorescence staining of TGR5 in the sciatic nerve of Lyz2-Cre mice treated with shControl virus or shGPBAR1 virus. Scale bar: 100 μm. (H) Analysis of the TGR5+ mean fluorescence density. n = 4 per group. $^{*}P < 0.05$; unpaired *t* test. (I) Comparisons of the 50% paw withdrawal threshold evaluated by the Von Frey test at POD7 between the shControl and the shGPBAR1 group. n = 8 to 9 per group. $^{*}P < 0.05$; 2-way ANOVA, Šídák post hoc test, $F(2, 45) = 6.523$, $F(2, 45) = 157.7$, $F(1, 45) = 4.323$. Data are presented as the mean ± SEM. ANOVA, analysis of variance; POD, postoperative day; pSNL, partial sciatic nerve ligation.

subjected to flow cytometry analysis. The results indicated that most of the GFP-labelled cells were CD11b+ (**Fig. 6B**). In addition, the GFP-labelled CD11b+ cells accounted for approximately 20% of the total CD11b+ cells (**Fig. 6C**). The knockdown efficiency of TGR5 in the sciatic nerve was further confirmed using RT-qPCR (**Fig. 6D**), Western blotting (**Figs. 6E and F**), and immunofluorescence staining (**Figs. 6G and H**). Von Frey tests carried out on POD7 and POD14 demonstrated that targeted knockdown of TGR5 in myeloid cells in the injured nerve site significantly exacerbated pSNL-induced mechanical allodynia (F (2, 45) = 6.523, F (2, 45) = 157.7, F (1, 45) = 4.32) (**Fig. 6I**). Similarly, compared with the shControl mice, mice in the shGPBAR1 group exhibited a significant escalation of spontaneous nocifensive behaviors (F (2, 45) = 3.293, F (2, 45) = 173.4, F (1, 45) = 9.682) (Fig. S7, available at http://links.lww.com/PAIN/C168). Overall, these results indicated that TGR5 expressed on myeloid cells in the sciatic nerve might play a protective role against pSNL-induced neuropathic pain.

3.7. Myeloid-cell-specific TGR5 knockdown induced significant upregulation of pro-inflammatory genes in the sciatic nerve

Although the contribution of myeloid cells to neuroinflammation has been well reported, whether the regulation of neuroinflammation is the main effect of myeloid TGR5 manipulation remains unknown. To screen the transcriptomic alterations induced by myeloid-cell-specific TGR5 knockdown, the sciatic nerves of Lyz2-Cre mice treated with shGPBAR1 or shControl virus at POD7 were subjected to bulk RNA-seq analysis.

Principal component analysis revealed distinct transcriptome characteristics between the 2 groups (**Fig. 7A**). A volcano map of the DEGs revealed that 5 and 77 genes were downregulated and upregulated, respectively, in the shGPBAR1 group compared with those in the shControl group (**Fig. 7B**). GO-enrichment analysis indicated that the top 5 biological processes involved by the upregulated genes were immune response, neutrophil chemotaxis, inflammatory response, immune system process, and chemotaxis. Specifically, several genes were involved in regulating NIK/NFκB signaling and the cytokine production process, especially the production process of TNF, IL-6, and IL-1β (**Fig. 7C**). The major pathways involved by the upregulated genes were further evaluated using KEGG-enrichment analysis. Cytokine and cytokine receptor interactions, as well as chemokine signaling, were the major enriched pathways. Similarly, genes in the NFκB, IL-17, NOD-like receptor, and TNF signaling pathways were significantly enriched (**Fig. 7D**). The expression of genes in the above enriched biological processes is indicated in the clustering heat map (**Fig. 7E**). Among these 24 DEGs, *Tnf*, *Il1b*, and *Nlrp3* were 3 key genes according to enrichment analysis. Furthermore, *Ccl3* and *Ccl4* were also among the cluster of 29 overlapping genes inversely regulated by pSNL and INT-777 treatment. The expression of these 5 genes was validated using RT-qPCR. Except for *Nlrp3*, the expression of the other 4 genes was significantly upregulated in the shGBAR1 group (**Figs. 7F–J**).

For the 5 downregulated DEGs, GO-enrichment analysis revealed that they were involved in dendritic spine morphogenesis, negative regulation of excitatory postsynaptic potential, and cellular response to nutrient levels (Fig. S8A, available at http://links.lww.com/PAIN/C168). Kyoto Encyclopedia of Genes and Genomes enrichment analysis implied that these genes were closely associated with axon guidance and neuroactive ligand-receptor interaction pathways (Fig. S8B, available at http://links.lww.com/PAIN/C168). The expression of genes in the above enriched biological processes is indicated in the clustering heat map (Fig. S8C, available at http://links.lww.com/PAIN/C168). Taken together, these results revealed that neuroinflammation is the primary biological process influenced by myeloid TGR5 knockdown, especially cytokine/chemokine signaling.

3.8. Myeloid-cell-specific TGR5 knockdown upregulated pro-inflammatory mediators and increased the proportion of monocytes/macrophages in the sciatic nerve

To confirm the effects of myeloid-cell-specific TGR5 knockdown on neuroinflammation-related alterations implied by the RNA-seq data, the protein levels of inflammatory mediators in the sciatic nerve were assessed at POD7. Cytometric bead array analysis indicated that the expression of CCL2, CCL3, TNF-α, and IL-6 was significantly upregulated in the shGPBAR1 group (**Figs. 8A–D**). The expression of CCL4 was not significantly different between the 2 groups, although the mRNA levels of *Ccl4* were significantly increased in the shGPBAR1 group (Fig. S9A, available at http://links.lww.com/PAIN/C168). The expression of CXCL9, CXCL10, and VEGF, which were upregulated by pSNL, were not altered by myeloid-cell-specific TGR5 knockdown (Figs. S9B–D, available at http://links.lww.com/PAIN/C168). Consistent with the effects of pSNL and TGR5 activation on the expression of IL-4, IL-10, IFN-α, and IFN-γ, TGR5 knockdown did not regulate their protein levels (Figs. S9E–H, available at http://links.lww.com/PAIN/C168).

The NLRP3-ASC inflammasome has been reported to regulate the generation of IL-1β.[29] Given the significant enrichment of DEGs in the NLRP3 regulation and IL-1β production pathways, their protein expression was assessed using Western blotting (**Fig. 8E**). The results indicated that the expression of NLRP3 was not significantly different between the shControl and shGPBAR1 groups, whereas the expressions of ASC, Caspase-1, and IL-1β were significantly upregulated by TGR5 knockdown (**Figs. 8F–I**). Furthermore, immunofluorescence staining indicated that NLRP3-ASC inflammasome and IL-1β colocalized with F480+ macrophages in the injured sciatic nerve at POD7 (**Figs. 8J and K**).

Based on the robust alterations of cytokines and chemokines induced by myeloid-cell-specific TGR5 knockdown, monocytes/macrophages in the sciatic nerve were evaluated using flow cytometry (**Fig. 9A**). The data revealed a significant increase in CD11b+ monocytes, F4/80+ macrophages, and CD11b+F4/80+ macrophages in the shGPBAR1 group compared with those in the shControl group (**Figs. 9B–D**). However, no significant differences were observed in the individual percentages of $CD86^{+}CD206-$ macrophages and CD86-CD206+ macrophages and the ratio of $CD86^{+}CD206-$ macrophages to CD86-CD206+ macrophages between the 2 groups (**Figs. 9E–G**).

These results confirmed the substantial regulatory impact of myeloid TGR5 on the expression of pro-inflammatory mediators and the proportion of monocytes/macrophages in the sciatic nerve. Taken together, the results suggested that myeloid-cell-specific TGR5 knockdown exaggerates neuroinflammation in the sciatic nerve after pSNL.

3.9. Activation of microglia in the dorsal horn of the spinal cord induced by partial sciatic nerve ligation was altered when TGR5 in the sciatic nerve was manipulated

Peripheral neuroinflammation contributes to central sensitization, which is the pivotal mechanism of neuropathic pain.[64]

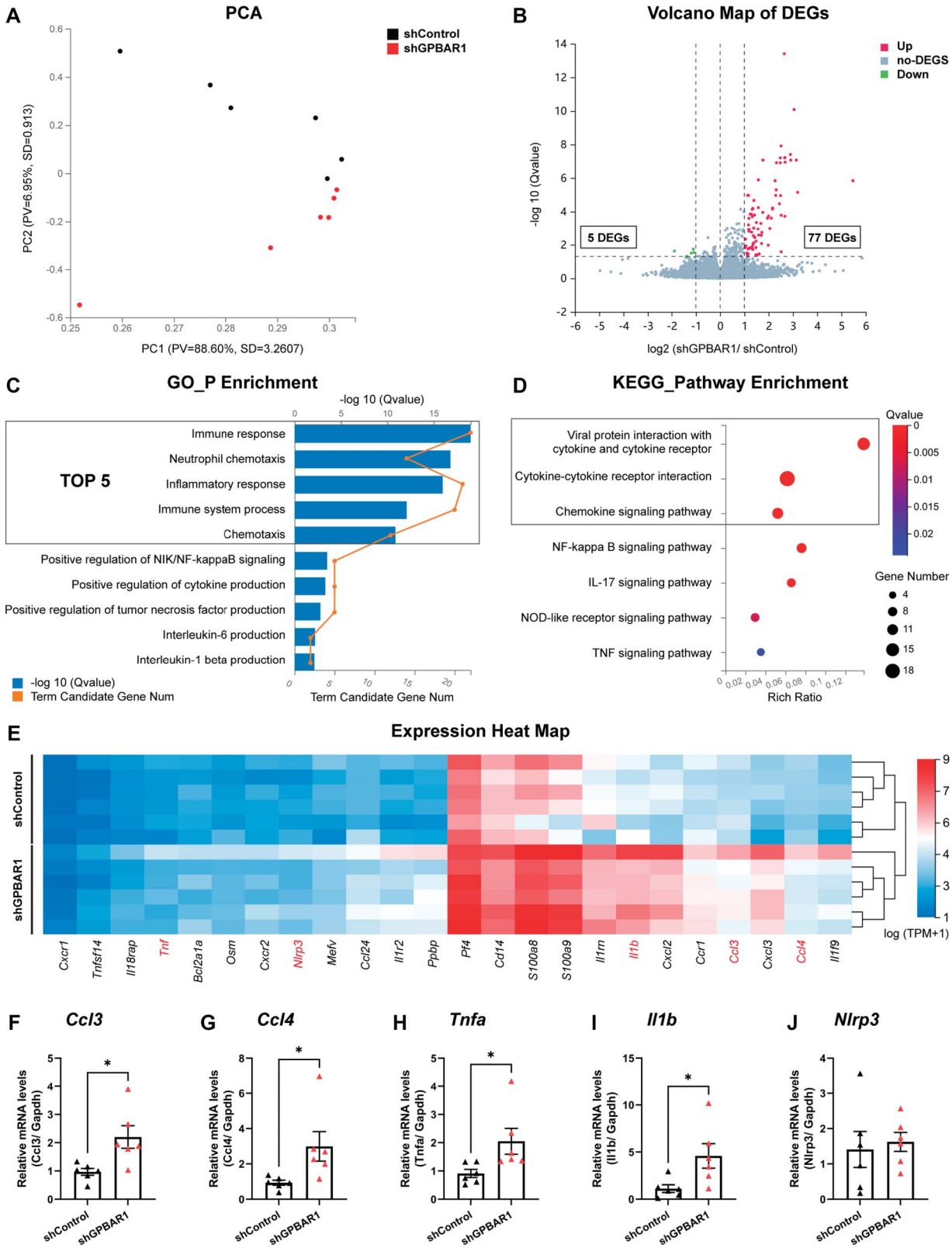

Figure 7. Transcriptome alterations in the sciatic nerve induced by myeloid-cell-specific TGR5 knockdown 7 days after pSNL. (A) PCA of the sciatic nerve in the shControl and shGPBAR1 groups at POD7. (B) Volcano plots of DEGs in the shGPBAR1 group compared with those in the shControl group, which included 77 upregulated and 5 downregulated genes, respectively. GO-enriched biological processes (C) and KEGG-enriched pathways (D) of 77 upregulated genes. (E) Heat map of DEGs involved in the production of cytokines. The gene expression of *Ccl3* (F), *Ccl4* (G), *Tnfα* (H), *Il1b* (I), and *Nlrp3* (J) were validated through RT-qPCR. n = 6 per group. $^*P < 0.05$; unpaired *t* test. Data are presented as the mean ± SEM. DEG, differentially expressed gene; GO, Gene Ontology; KEGG, Kyoto Encyclopedia of Genes and Genomes; PCA, principal component analysis; RT-qPCR, real-time quantitative PCR.

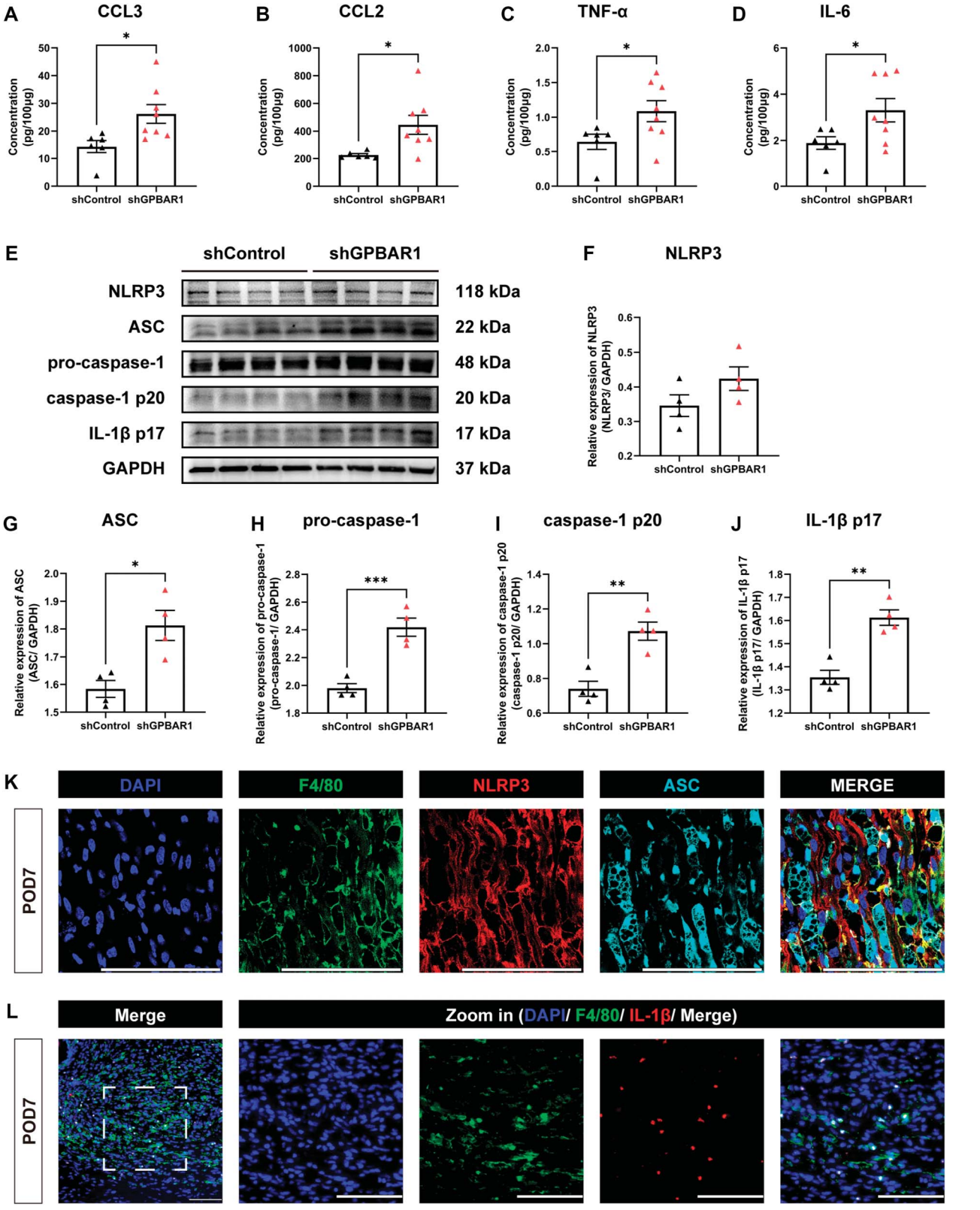

Figure 8. Effects of myeloid-cell-specific TGR5 knockdown on the expression of inflammatory mediators 7 days after pSNL. Protein levels of CCL3 (A), CCL2 (B), TNF-α (C), and IL-6 (D) in the sciatic nerve at POD7 were measured using cytometric bead array analysis. n = 6 to 8 per group. $^{*}P < 0.05$; unpaired *t* test. Representative Western blotting bands (E) and densitometric quantification of NLRP3 (F), ASC (G), pro-caspase-1 (H), caspase-1 p20 (I), and IL-1β p17 (J) in the sciatic nerve of Lyz2-Cre mice treated with shControl virus or shGPBAR1 virus. n = 4 per group. $^{*}P < 0.05$, $^{**}P < 0.01$, $^{***}P < 0.001$; unpaired *t* test. Data are presented as the mean ± SEM. (K) Representative microphotographs showing immunofluorescence staining of F4/80 (green), NLRP3 (red), and ASC (cyan) in the sciatic nerve after pSNL. Nuclei were stained with DAPI (blue). Scale bar: 100 μm. (L) Representative microphotographs showing immunofluorescence staining of F4/80 (green) and IL-1β (red) in the sciatic nerve after pSNL. Nuclei were stained with DAPI (blue). Scale bar: 100 μm. DAPI, 4′,6-diamidino-2-phenylindole; POD, postoperative day; pSNL, partial sciatic nerve ligation.

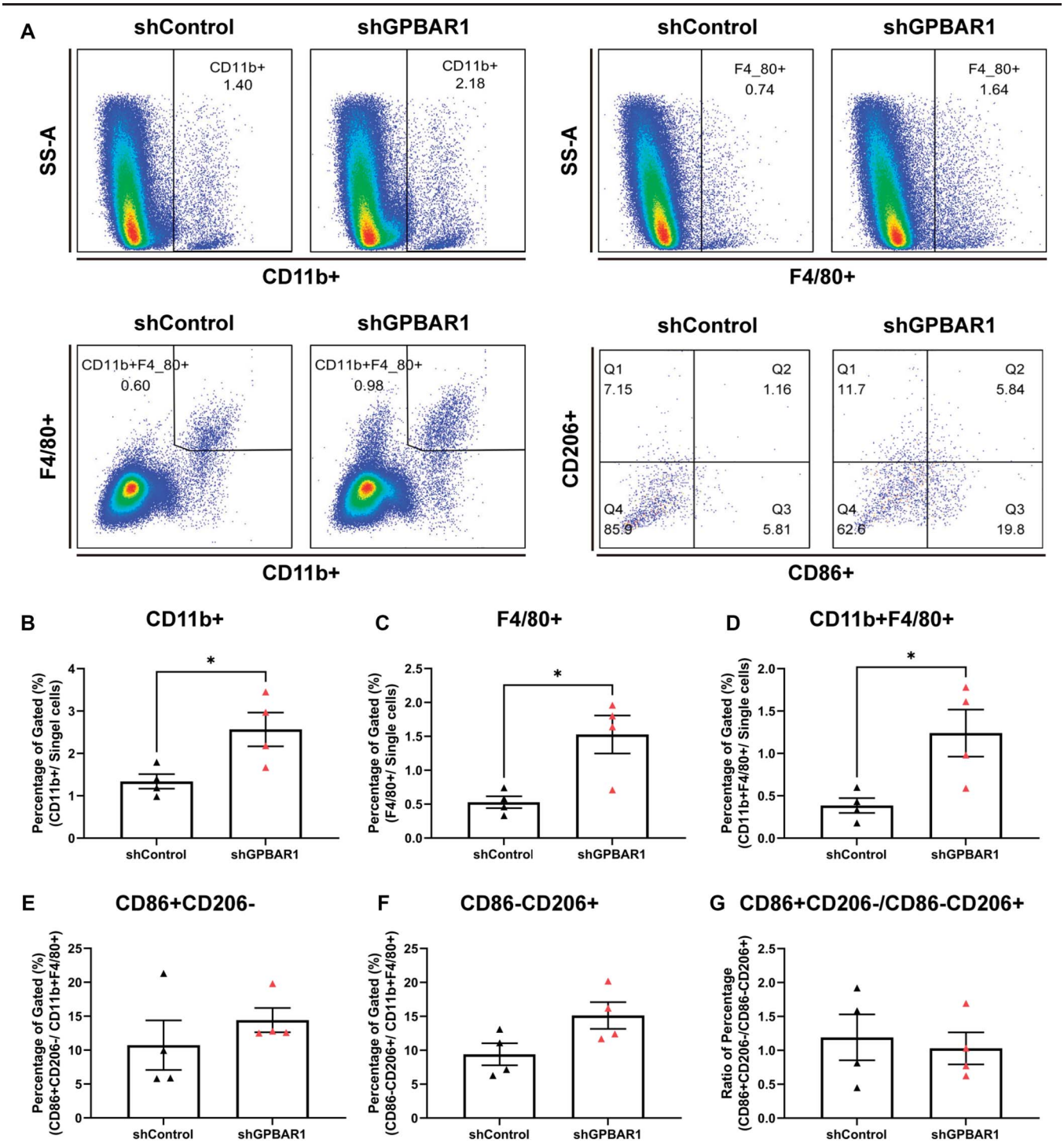

Figure 9. Effects of myeloid-cell-specific TGR5 knockdown on alterations of macrophages 7 days after pSNL. (A) Representative flow cytometry pseudocolor dot plots of myeloid cell populations in the sciatic nerve of mice treated with shControl virus or shGPBAR1 virus at POD7. Percentages of CD11b+ cells (B), F4/80+ cells (C), and CD11b+F4/80+ cells (D) among single cells defined by FS-A and FS-W. Percentages of $CD86^{+}CD206-$ cells (E) and CD86-CD206+ cells (F) among CD11b+F4/80+ cells. (G) The ratio of $CD86^{+}CD206-$ macrophages to CD86-CD206+ macrophages. n = 4 per group; $^{*}P < 0.05$; unpaired *t* test. Data are presented as the mean ± SEM. POD, postoperative day; pSNL, partial sciatic nerve ligation.

To estimate the effects of TGR5 manipulation on central sensitization in the spinal cord level, the activation of microglia, indicated with the Iba-1 positive area in the ipsilateral dorsal horn of spinal cord induced by pSNL was analyzed at POD7 and POD14. Immunofluorescence staining indicated that the activation of microglia was decreased by perisciatic nerve INT-777 treatment (**Figs. 10A–C**) and was increased by myeloid-cell-specific TGR5 knockdown in the sciatic nerve compared with their respective control groups (**Figs. 10D–F**).

4. Discussion

In this study, we confirmed that the activation of TGR5 in the injured nerve site mitigates pSNL-induced neuropathic pain by modulating neuroinflammation. Specifically, the expression of

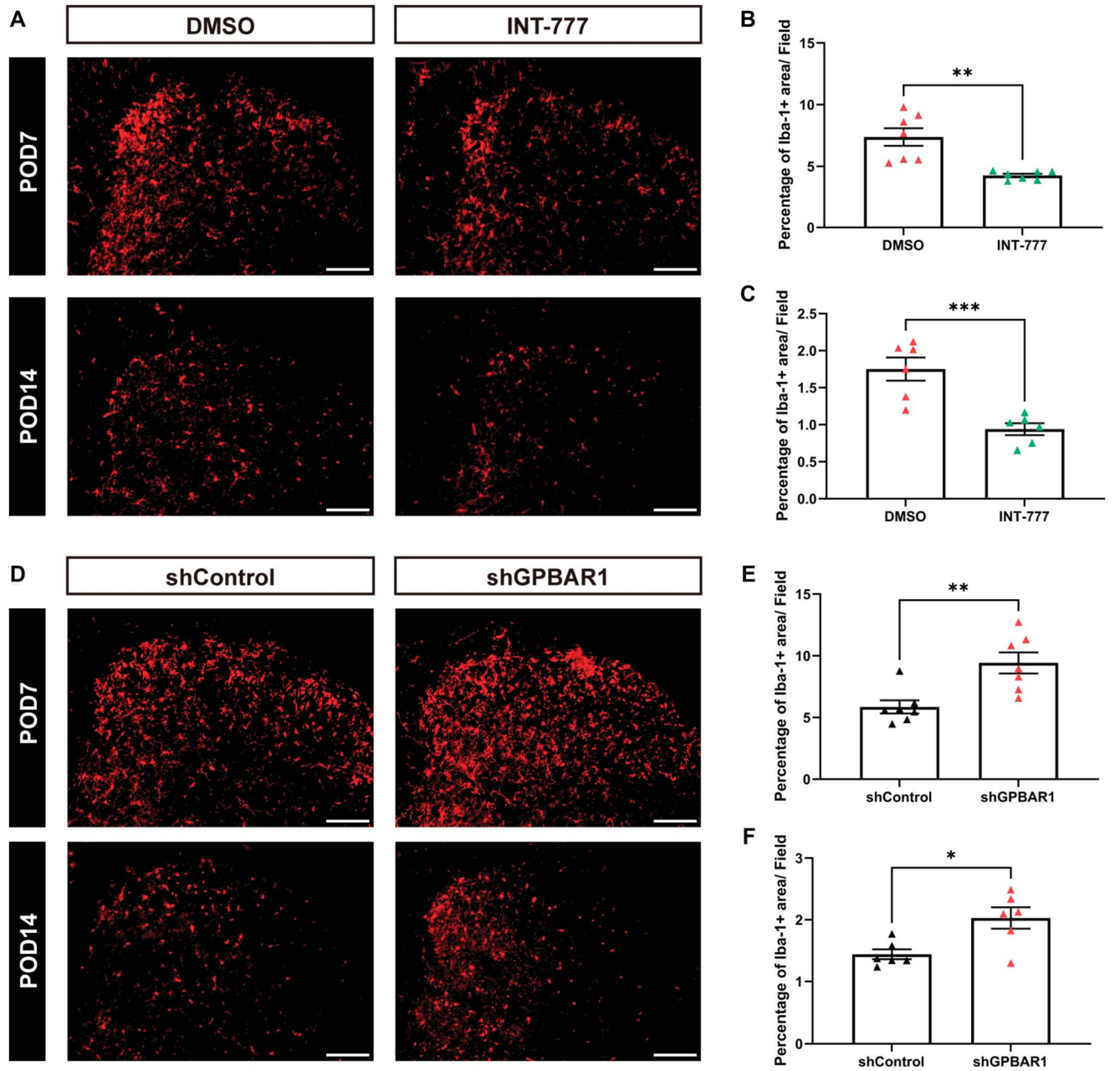

Figure 10. Effects of TGR5 manipulations on microglia activation in the spinal cord after pSNL. (A) Representative microphotographs of immunofluorescence staining of Iba-1 in the ipsilateral dorsal horn of the spinal cord of mice treated with DMSO or INT-777 at POD7 and POD14. Scale bar: 100 μm. Analysis of the percentage of Iba-1+ area on POD7 (B) and POD14 (C). n = 6 to 7 per group. $^{**}P < 0.01$, $^{***}P < 0.001$; unpaired *t* test. (D) Representative microphotographs of immunofluorescence staining of Iba-1 in the ipsilateral dorsal horn of the spinal cord of mice treated with shControl virus or shGPBAR1 virus. Scale bar: 100 μm. Analysis of the percentage of Iba-1+ area on POD7 (E) and POD14 (F). n = 6 to 7 per group. $^{*}P < 0.05$, $^{**}P < 0.01$; unpaired *t* test. Data are presented as the mean ± SEM. DMSO, dimethylsulfoxide; Iba-1, ionized calcium-binding adapter molecule 1; POD, postoperative day; pSNL, partial sciatic nerve ligation.

TGR5 increased in the injured nerve site, and local administration of a TGR5 agonist, following a prevention protocol, alleviated mechanical allodynia and spontaneous pain by preventing the increase of pro-inflammatory cytokines/chemokines and monocytes/macrophages induced by pSNL. By contrast, specific knockdown of TGR5 in myeloid cells, also following a prevention protocol, exacerbated neuropathic pain by increasing the expression of pro-inflammatory mediators and the proportion of monocytes/macrophages.

TGR5, a G-protein-coupled receptor, is abundantly expressed in the gallbladder epithelium and is minimally to moderately expressed in almost all other tissues and cell types.[61] In the nervous system, TGR5 is found in both neurons and nonneuronal cells, including resident and infiltrating immune cells.[38] The distinct functions of TGR5 in neurons and nonneuronal cells have been previously reported. In neurons, the administration of a TGR5 agonist increases the intrinsic excitability of dorsal root ganglion (DRG) neurons and activates colon-innervating DRG neurons isolated from naïve mice.[1,8] In nonneuronal cells, TGR5 activation mitigates LPS-induced inflammatory responses in both microglia and macrophages.[23,70] Moreover, the established pain modulation roles of TGR5 expressed in different anatomical regions are inconsistent. In a mouse model of paclitaxel-induced peripheral neuropathic pain, TGR5 expressed in DRG neurons

contributed to the upregulation of CCR5 and then mediated deoxycholic acid–induced mechanical allodynia.[74] In a mouse model of spared nerve injury–induced neuropathic pain, intrathecal injection of TGR5 agonist alleviated mechanical allodynia by inhibiting the activation of glial cells and modulating the function of $GABA_A$ receptors in the spinal cord.[67] In this study, TGR5 in the injured sciatic nerve was mainly expressed in the macrophages, and pSNL-induced neuropathic pain was significantly alleviated by perisciatic administration of the TGR5-specific agonist, INT-777, following a prevention protocol. The molecular mechanism underlying this TGR5-activation-regulated phenotype is more likely to consist of a negative regulation effect on inflammation rather than a positive impact on neuron excitability. This inference was validated through bulk RNA-seq analysis of injured nerve tissues. The sequence data indicated that, among all changes in the transcriptome, the inflammatory response is the primary process related to the DEGs , which were inversely regulated by pSNL and TGR5 activation. In addition, pSNL-induced mechanical allodynia and spontaneous pain were further exaggerated when TGR5 was specifically knocked down in myeloid cells, and transcriptomic alterations were predominantly related to the inflammatory response. Overall, these data demonstrated that increased TGR5 in the injured sciatic nerve serves as a molecular target for modulating pSNL-induced neuropathic pain by regulating neuroinflammation. However, the specific expression of TGR5 in nerve fibers and its potential roles in pain modulation were not assessed in this study, warranting further research.

In the field of neuropathic pain, ample evidence has underscored the substantial role of neuroinflammation in driving both peripheral and central sensitization, thereby enhancing pain hypersensitivity.[4,20] Recent findings have indicated that specific subsets of immune cells contribute to the alleviation of neuropathic pain.[19] Among them, macrophages are a subset of cells that exhibit remarkable plasticity and adopt functionally distinct phenotypes.[44] Although the phenotypes of macrophages observed in vivo are not as distinct as those found in vitro,[42] some molecules reflect the possible functions of specific populations of macrophages, such as CD86 (a pro-inflammatory response–associated costimulatory molecule expressed by antigen-presenting cells)[12] and CD206 (an anti-inflammatory response–associated mannose receptor).[58] Inflammatory mediators that are highly expressed by pro-inflammatory macrophages, such as IL-1β,[5] IL-6,[40] and TNF-α,[31] have been reported to induce neuronal sensitization and circulating leukocyte recruitment into inflamed tissue.[62] The anti-nociceptive properties of the mediators secreted by anti-inflammatory macrophages, such as IL-10[35,47] and IL-4,[9,36] have also been validated. In this study, we confirmed such dynamic changes in macrophages as well as their proximity to neuron fibers in the injured nerve site. In the context of TGR5 manipulation, alongside changes in mechanical allodynia and spontaneous nocifensive behaviors, there was a significant regulation of pro-inflammatory mediators and the proportion of monocytes/macrophages in the sciatic nerve at POD7. However, no significant differences were observed in the expression of anti-inflammatory mediators. Activation of microglia in the spinal dorsal horn is an important part of central sensitization and is known to contribute to neuropathic pain.[26] In this study, manipulations of TGR5 in the sciatic nerve significantly altered the activation level of microglia. Overall, the high relevance between macrophage-mediated neuroinflammation and pSNL-induced neuropathic pain was further confirmed in this study. Regarding the neuronal mechanisms that mediate the effect of TGR5-modulated neuroinflammation on pain perception, although 5 genes involved in dendritic spine morphogenesis and negative regulation of the excitatory post-synaptic process were found to be downregulated by TGR5 knockdown, the specific roles of these genes remain to be further investigated.

Since its detection, the modulatory effects of TGR5 on the functions of monocytes and macrophages have been extensively studied. Specifically, the production of pro-inflammatory cytokines in macrophages, such as TNF-α, IL-6, and IL-1β, has been reported to be inhibited by TGR5 activation through the NF-κB pathway[50,69] and to be exacerbated by TGR5 deficiency through stabilization of the β-catenin destruction complex.[52] The production of anti-inflammatory cytokines, such as IL-4 and IL-10, has been reported to be upregulated by macrophage TGR5 activation; however, whether the presence of TGR5 is indispensable for the polarization of anti-inflammatory M2-like macrophages remains under debate.[49,73] The expressions of chemokines, such as CCL2, CCL3, and CCL4, are also regulated by TGR5. In the presence of LPS, TGR5 deficiency exaggerates the upregulation of chemokines, whereas TGR5 activation has the opposite effect on macrophages through the mTOR–C/EBPβ pathway.[49] In addition, the activation of the NLRP3 inflammasome is inhibited by bile acids through the TGR5–cAMP–PKA axis,[22] and TGR5 deficiency exaggerates the inflammatory response of macrophages stimulated with palmitic acid by promoting the activation of the NLRP3 inflammasome.[56] In this study, the increase of pro-inflammatory cytokines TNF-α, IL-6, and IL-1β as well as that of chemokines CCL3 and CCL2 in the sciatic nerve were exacerbated by myeloid-cell-specific TGR5 knockdown. These results are consistent with the known effects of TGR5 on macrophages. Regarding the NLRP3 inflammasome, although the expression of NLRP3 was unaltered, the expression of the adaptor protein ASC, which connects the inflammasome sensor molecule to Caspase-1, as well as that of Caspase-1, which initiates downstream responses, were significantly upregulated by TGR5 knockdown, indicating the further activation of the NLRP3 inflammasome. As for the specific molecular pathways underlying the modulation of inflammatory mediators in macrophages by TGR5, itself located in the injured sciatic nerve, further research is needed to unveil the intrinsic cell alterations in situ rather than the changes induced by mimicking the inflammatory response in cell experiments.

Regarding the experimental findings of this study, although the targeted knockdown of TGR5 in myeloid cells exacerbated neuropathic pain, the increase in TGR5 expression following nerve injury alone apparently did not suffice to impede pain progression. Alleviation of neuropathic pain was solely observed upon administration of exogenous TGR5 agonists, underscoring the pivotal regulatory role of endogenous ligands in TGR5 function. The endogenous ligands of TGR5 are primary bile acids synthesized from cholesterol and secondary bile acids metabolized by the gut microbiota, as well as some neurosteroids.[11,33] The majority of bile acids are generated and exist in the enterohepatic system, and a minority of them spill over into the circulation.[48] In the peripheral and central nervous systems, the presence of bile acids has been confirmed.[68] In addition to being transported from the circulation, bile acids are also synthesized locally in the brain and the spinal cord, as evidenced by the detection of rate-limiting enzymes for synthesis.[25] In this study, bulk RNA-seq data indicated that genes involved in the biosynthesis and metabolism of cholesterol were significantly regulated in the sciatic nerve after pSNL, implying the potential alterations of endogenous TGR5 ligands. However, whether the protein levels of bile acids in the injured sciatic nerve change, and

whether these ligands participate in the modulation of pathological neuropathic pain processes, should be further studied.

The primary limitation of this study is the use of only male mice. Given the well-documented sex differences in neuroinflammatory mechanisms,[13,21] whether TGR5 plays the same regulatory role in neuroinflammation and mechanical allodynia in female mice remains unknown.

In conclusion, this study demonstrated that neuropathic pain is significantly reduced when a TGR5 agonist is administered following a prevention protocol. The protective effect seems to stem from the reduction of neuroinflammation by modulating the expression of inflammatory mediators induced by pSNL. Thus, TGR5, which acts at the site of peripheral nerve injury, emerges as a promising target for treating neuropathic pain. However, further studies are warranted to confirm these findings using an intervention protocol with a TGR5 agonist.

Conflict of interest statement

The authors have no conflicts of interest to declare.

Acknowledgements

This study was supported by the National Natural Science Foundation of China (grant numbers 81870788, 82170979, 82371227, 82171226, 81974169, and 82001192) and the Natural Science Foundation of Beijing Municipality (grant number 7222105).

Ethics approval statement: The animal study protocol was approved by the Ethics Committee of the Peking University Health Science Center (protocol code: LA2018041).

Data availability statement: All data are available upon request.

Supplemental digital content

Supplemental digital content associated with this article can be found online at http://links.lww.com/PAIN/C168.

Article history:
Received 9 July 2024
Received in revised form 18 September 2024
Accepted 22 September 2024
Available online 25 October 2024

References

[1] Alemi F, Kwon E, Poole DP, Lieu T, Lyo V, Cattaruzza F, Cevikbas F, Steinhoff M, Nassini R, Materazzi S, Guerrero-Alba R, Valdez-Morales E, Cottrell GS, Schoonjans K, Geppetti P, Vanner SJ, Bunnett NW, Corvera CU. The TGR5 receptor mediates bile acid-induced itch and analgesia. J Clin Invest 2013;123:1513–30.
[2] Bannister K, Sachau J, Baron R, Dickenson AH. Neuropathic pain: mechanism-based therapeutics. Annu Rev Pharmacol Toxicol 2020;60:257–74.
[3] Baron R, Binder A, Wasner G. Neuropathic pain: diagnosis, pathophysiological mechanisms, and treatment. Lancet Neurol 2010;9:807–19.
[4] Bethea JR, Fischer R. Role of peripheral immune cells for development and recovery of chronic pain. Front Immunol 2021;12:641588.
[5] Binshtok AM, Wang H, Zimmermann K, Amaya F, Vardeh D, Shi L, Brenner GJ, Ji RR, Bean BP, Woolf CJ, Samad TA. Nociceptors are interleukin-1beta sensors. J Neurosci 2008;28:14062–73.
[6] Bouhassira D, Attal N. Translational neuropathic pain research: a clinical perspective. Neuroscience 2016;338:27–35.
[7] Callahan BL, Gil AS, Levesque A, Mogil JS. Modulation of mechanical and thermal nociceptive sensitivity in the laboratory mouse by behavioral state. J Pain 2008;9:174–84.
[8] Castro J, Harrington AM, Lieu T, Garcia-Caraballo S, Maddern J, Schober G, O'Donnell T, Grundy L, Lumsden AL, Miller P, Ghetti A, Steinhoff MS, Poole DP, Dong X, Chang L, Bunnett NW, Brierley SM. Activation of pruritogenic TGR5, MrgprA3, and MrgprC11 on colon-innervating afferents induces visceral hypersensitivity. JCI Insight 2019;4:e131712.
[9] Celik MO, Labuz D, Keye J, Glauben R, Machelska H. IL-4 induces M2 macrophages to produce sustained analgesia via opioids. JCI Insight 2020;5:e133093.
[10] Chaplan SR, Bach FW, Pogrel JW, Chung JM, Yaksh TL. Quantitative assessment of tactile allodynia in the rat paw. J Neurosci Methods 1994;53:55–63.
[11] Collins SL, Stine JG, Bisanz JE, Okafor CD, Patterson AD. Bile acids and the gut microbiota: metabolic interactions and impacts on disease. Nat Rev Microbiol 2023;21:236–47.
[12] Cutolo M, Nadler SG. Advances in CTLA-4-Ig-mediated modulation of inflammatory cell and immune response activation in rheumatoid arthritis. Autoimmun Rev 2013;12:758–67.
[13] del Rivero T, Fischer R, Yang F, Swanson KA, Bethea JR. Tumor necrosis factor receptor 1 inhibition is therapeutic for neuropathic pain in males but not in females. PAIN 2018;160:922–31.
[14] Deuis JR, Dvorakova LS, Vetter I. Methods used to evaluate pain behaviors in rodents. Front Mol Neurosci 2017;10:284.
[15] Dixon WJ. Efficient analysis of experimental observations. Annu Rev Pharmacol Toxicol 1980;20:441–62.
[16] Domoto R, Sekiguchi F, Tsubota M, Kawabata A. Macrophage as a peripheral pain regulator. Cells 2021;10:1881.
[17] Donnelly CR, Chen O, Ji RR. How do sensory neurons sense danger signals? Trends Neurosciences 2020;43:822–38.
[18] Ellis A, Bennett DLH. Neuroinflammation and the generation of neuropathic pain. Br J Anaesth 2013;111:26–37.
[19] Fiore NT, Debs SR, Hayes JP, Duffy SS, Moalem-Taylor G. Pain-resolving immune mechanisms in neuropathic pain. Nat Rev Neurol 2023;19:199–220.
[20] Grace PM, Hutchinson MR, Maier SF, Watkins LR. Pathological pain and the neuroimmune interface. Nat Rev Immunol 2014;14:217–31.
[21] Gregus AM, Levine IS, Eddinger KA, Yaksh TL, Buczynski MW. Sex differences in neuroimmune and glial mechanisms of pain. PAIN 2021;162:2186–200.
[22] Guo C, Xie S, Chi Z, Zhang J, Liu Y, Zhang L, Zheng M, Zhang X, Xia D, Ke Y, Lu L, Wang D. Bile acids control inflammation and metabolic disorder through inhibition of NLRP3 inflammasome. Immunity 2016;45:802–16.
[23] Hogenauer K, Arista L, Schmiedeberg N, Werner G, Jaksche H, Bouhelal R, Nguyen DG, Bhat BG, Raad L, Rauld C, Carballido JM. G-protein-coupled bile acid receptor 1 (GPBAR1, TGR5) agonists reduce the production of proinflammatory cytokines and stabilize the alternative macrophage phenotype. J Med Chem 2014;57:10343–54.
[24] Hu X, Yan J, Huang L, Araujo C, Peng J, Gao L, Liu S, Tang J, Zuo G, Zhang JH. INT-777 attenuates NLRP3-ASC inflammasome-mediated neuroinflammation via TGR5/cAMP/PKA signaling pathway after subarachnoid hemorrhage in rats. Brain Behav Immun 2021;91:587–600.
[25] Hurley MJ, Bates R, Macnaughtan J, Schapira AHV. Bile acids and neurological disease. Pharmacol Ther 2022;240:108311.
[26] Inoue K, Tsuda M. Microglia in neuropathic pain: cellular and molecular mechanisms and therapeutic potential. Nat Rev Neurosci 2018;19:138–52.
[27] Iwai H, Ataka K, Suzuki H, Dhar A, Kuramoto E, Yamanaka A, Goto T. Tissue-resident M2 macrophages directly contact primary sensory neurons in the sensory ganglia after nerve injury. J Neuroinflammation 2021;18:227.
[28] Ji RR, Chamessian A, Zhang YQ. Pain regulation by non-neuronal cells and inflammation. Science 2016;354:572–7.
[29] Jia M, Wu C, Gao F, Xiang H, Sun N, Peng P, Li J, Yuan X, Li H, Meng X, Tian B, Shi J, Li M. Activation of NLRP3 inflammasome in peripheral nerve contributes to paclitaxel-induced neuropathic pain. Mol Pain 2017;13:1744806917719804.
[30] Jin P, Deng S, Tian M, Lenahan C, Wei P, Wang Y, Tan J, Wen H, Zhao F, Gao Y, Gong Y. INT-777 prevents cognitive impairment by activating Takeda G protein-coupled receptor 5 (TGR5) and attenuating neuroinflammation via cAMP/PKA/CREB signaling axis in a rat model of sepsis. Exp Neurol 2021;335:113504.
[31] Jin X, Gereau RW. Acute p38-mediated modulation of tetrodotoxin-resistant sodium channels in mouse sensory neurons by tumor necrosis factor-alpha. J Neurosci 2006;26:246–55.
[32] Kawamata Y, Fujii R, Hosoya M, Harada M, Yoshida H, Miwa M, Fukusumi S, Habata Y, Itoh T, Shintani Y, Hinuma S, Fujisawa Y, Fujino M. A G protein-coupled receptor responsive to bile acids. J Biol Chem 2003;278:9435–40.
[33] Keitel V, Görg B, Bidmon HJ, Zemtsova I, Spomer L, Zilles K, Häussinger D. The bile acid receptor TGR5 (Gpbar-1) acts as a neurosteroid receptor in brain. Glia 2010;58:1794–805.

[34] Kiguchi N, Maeda T, Kobayashi Y, Fukazawa Y, Kishioka S. Macrophage inflammatory protein-1alpha mediates the development of neuropathic pain following peripheral nerve injury through interleukin-1beta up-regulation. PAIN 2010;149:305–15.
[35] Kwilasz AJ, Green Fulgham SM, Ellis A, Patel HP, Duran-Malle JC, Favret J, Harvey LO Jr, Rieger J, Maier SF, Watkins LR. A single peri-sciatic nerve administration of the adenosine 2A receptor agonist ATL313 produces long-lasting anti-allodynia and anti-inflammatory effects in male rats. Brain Behav Immun 2019;76:116–25.
[36] Labuz D, Celik MO, Seitz V, Machelska H. Interleukin-4 induces the release of opioid peptides from M1 macrophages in pathological pain. J Neurosci 2021;41:2870–82.
[37] Liang YJ, Feng SY, Qi YP, Li K, Jin ZR, Jing HB, Liu LY, Cai J, Xing GG, Fu KY. Contribution of microglial reaction to increased nociceptive responses in high-fat-diet (HFD)-induced obesity in male mice. Brain Behav Immun 2019;80:777–92.
[38] Lieu T, Jayaweera G, Bunnett NW. GPBA: a GPCR for bile acids and an emerging therapeutic target for disorders of digestion and sensation. Br J Pharmacol 2014;171:1156–66.
[39] Liu L, Yin Y, Li F, Malhotra C, Cheng J. Flow cytometry analysis of inflammatory cells isolated from the sciatic nerve and DRG after chronic constriction injury in mice. J Neurosci Methods 2017;284:47–56.
[40] Liu Q, Chen W, Fan X, Wang J, Fu S, Cui S, Liao F, Cai J, Wang X, Huang Y, Su L, Zhong L, Yi M, Liu F, Wan Y. Upregulation of interleukin-6 on Cav3.2 T-type calcium channels in dorsal root ganglion neurons contributes to neuropathic pain in rats with spinal nerve ligation. Exp Neurol 2019;317:226–43.
[41] Malmberg AB, Basbaum AI. Partial sciatic nerve injury in the mouse as a model of neuropathic pain: behavioral and neuroanatomical correlates. PAIN 1998;76:215–22.
[42] Martinez FO, Gordon S. The M1 and M2 paradigm of macrophage activation: time for reassessment. F1000Prime Rep 2014;6:13.
[43] McMahon SB, La Russa F, Bennett DL. Crosstalk between the nociceptive and immune systems in host defence and disease. Nat Rev Neurosci 2015;16:389–402.
[44] Mosser DM, Hamidzadeh K, Goncalves R. Macrophages and the maintenance of homeostasis. Cell Mol Immunol 2021;18:579–87.
[45] Msheik Z, El Massry M, Rovini A, Billet F, Desmoulière A. The macrophage: a key player in the pathophysiology of peripheral neuropathies. J Neuroinflammation 2022;19:97.
[46] Nelson TS, Sinha GP, Santos DFS, Jukkola P, Prasoon P, Winter MK, McCarson KE, Smith BN, Taylor BK. Spinal neuropeptide Y Y1 receptor-expressing neurons are a pharmacotherapeutic target for the alleviation of neuropathic pain. Proc Natl Acad Sci U S A 2022;119:e2204515119.
[47] Niehaus JK, Taylor-Blake B, Loo L, Simon JM, Zylka MJ. Spinal macrophages resolve nociceptive hypersensitivity after peripheral injury. Neuron 2021;109:1274–82.e6.
[48] Perino A, Demagny H, Velazquez-Villegas L, Schoonjans K. Molecular physiology of bile acid signaling in health, disease, and aging. Physiol Rev 2021;101:683–731.
[49] Perino A, Pols TW, Nomura M, Stein S, Pellicciari R, Schoonjans K. TGR5 reduces macrophage migration through mTOR-induced C/EBPβ differential translation. J Clin Invest 2014;124:5424–36.
[50] Pols TW, Nomura M, Harach T, Lo Sasso G, Oosterveer MH, Thomas C, Rizzo G, Gioiello A, Adorini L, Pellicciari R, Auwerx J, Schoonjans K. TGR5 activation inhibits atherosclerosis by reducing macrophage inflammation and lipid loading. Cell Metab 2011;14:747–57.
[51] Raja SN, Carr DB, Cohen M, Finnerup NB, Flor H, Gibson S, Keefe FJ, Mogil JS, Ringkamp M, Sluka KA, Song XJ, Stevens B, Sullivan MD, Tutelman PR, Ushida T, Vader K. The revised International Association for the Study of Pain definition of pain: concepts, challenges, and compromises. PAIN 2020;161:1976–82.
[52] Rao J, Yang C, Yang S, Lu H, Hu Y, Lu L, Cheng F, Wang X. Deficiency of TGR5 exacerbates immune-mediated cholestatic hepatic injury by stabilizing the β-catenin destruction complex. Int Immunol 2020;32: 321–34.
[53] Rice ASC, Smith BH, Blyth FM. Pain and the global burden of disease. PAIN 2016;157:791–6.
[54] Scholz J, Finnerup NB, Attal N, Aziz Q, Baron R, Bennett MI, Benoliel R, Cohen M, Cruccu G, Davis KD, Evers S, First M, Giamberardino MA, Hansson P, Kaasa S, Korwisi B, Kosek E, Lavand'homme P, Nicholas M, Nurmikko T, Perrot S, Raja SN, Rice ASC, Rowbotham MC, Schug S, Simpson DM, Smith BH, Svensson P, Vlaeyen JWS, Wang SJ, Barke A, Rief W, Treede RD; Classification Committee of the Neuropathic Pain Special Interest Group NeuPSIG. The IASP classification of chronic pain for ICD-11: chronic neuropathic pain. PAIN 2019;160:53–9.
[55] Seltzer Z, Dubner R, Shir Y. A novel behavioral model of neuropathic pain disorders produced in rats by partial sciatic nerve injury. PAIN 1990;43: 205–18.
[56] Shi Y, Su W, Zhang L, Shi C, Zhou J, Wang P, Wang H, Shi X, Wei S, Wang Q, Auwerx J, Schoonjans K, Yu Y, Pan R, Zhou H, Lu L. TGR5 regulates macrophage inflammation in nonalcoholic steatohepatitis by modulating NLRP3 inflammasome activation. Front Immunol 2020;11:609060.
[57] Tanaka T, Okuda H, Isonishi A, Terada Y, Kitabatake M, Shinjo T, Nishimura K, Takemura S, Furue H, Ito T, Tatsumi K, Wanaka A. Dermal macrophages set pain sensitivity by modulating the amount of tissue NGF through an SNX25–Nrf2 pathway. Nat Immunol 2023;24:439–51.
[58] Tang PMK, Nikolic-Paterson DJ, Lan HY. Macrophages: versatile players in renal inflammation and fibrosis. Nat Rev Nephrol 2019;15:144–58.
[59] Thacker MA, Clark AK, Marchand F, McMahon SB. Pathophysiology of peripheral neuropathic pain: immune cells and molecules. Anesth Analg 2007;105:838–47.
[60] van Hecke O, Austin SK, Khan RA, Smith BH, Torrance N. Neuropathic pain in the general population: a systematic review of epidemiological studies. PAIN 2014;155:654–62.
[61] Vassileva G, Golovko A, Markowitz L, Abbondanzo SJ, Zeng M, Yang S, Hoos L, Tetzloff G, Levitan D, Murgolo NJ, Keane K, Davis HR Jr, Hedrick J, Gustafson EL. Targeted deletion of Gpbar1 protects mice from cholesterol gallstone formation. Biochem J 2006;398:423–30.
[62] Wang Y, Guo L, Yin X, McCarthy EC, Cheng MI, Hoang AT, Chen HC, Patel AY, Allard Trout D, Xu E, Yakobian N, Hugo W, Howard JF, Sheu KM, Hoffmann A, Lechner MG, Su MA. Pathogenic TNF-α drives peripheral nerve inflammation in an Aire-deficient model of autoimmunity. Proc Natl Acad Sci U S A 2022;119:e2114406119.
[63] Williams NH, Lewis R, Din NU, Matar HE, Fitzsimmons D, Phillips CJ, Sutton A, Burton K, Hendry M, Nafees S, Wilkinson C. A systematic review and meta-analysis of biological treatments targeting tumour necrosis factor α for sciatica. Eur Spine J 2013;22:1921–35.
[64] Woolf CJ, Salter MW. Neuronal plasticity: increasing the gain in pain. Science 2000;288:1765–9.
[65] Wu X, Liu C, Chen L, Du YF, Hu M, Reed MN, Long Y, Suppiramaniam V, Hong H, Tang SS. Protective effects of tauroursodeoxycholic acid on lipopolysaccharide-induced cognitive impairment and neurotoxicity in mice. Int Immunopharmacol 2019;72:166–75.
[66] Wu X, Lv YG, Du YF, Hu M, Reed MN, Long Y, Suppiramaniam V, Hong H, Tang SS. Inhibitory effect of INT-777 on lipopolysaccharide-induced cognitive impairment, neuroinflammation, apoptosis, and synaptic dysfunction in mice. Prog Neuropsychopharmacol Biol Psychiatry 2019;88:360–74.
[67] Wu Y, Qiu Y, Su M, Wang L, Gong Q, Wei X. Activation of the bile acid receptors TGR5 and FXR in the spinal dorsal horn alleviates neuropathic pain. CNS Neurosci Ther 2023;29:1981–98.
[68] Xing C, Huang X, Wang D, Yu D, Hou S, Cui H, Song L. Roles of bile acids signaling in neuromodulation under physiological and pathological conditions. Cell Biosci 2023;13:106.
[69] Yang H, Zhou H, Zhuang L, Auwerx J, Schoonjans K, Wang X, Feng C, Lu L. Plasma membrane-bound G protein-coupled bile acid receptor attenuates liver ischemia/reperfusion injury via the inhibition of toll-like receptor 4 signaling in mice. Liver Transpl 2017;23:63–74.
[70] Yanguas-Casas N, Barreda-Manso MA, Nieto-Sampedro M, Romero-Ramirez L. TUDCA: an agonist of the bile acid receptor GPBAR1/TGR5 with anti-inflammatory effects in microglial cells. J Cell Physiol 2017;232:2231–45.
[71] Yao Y, Echeverry S, Shi XQ, Yang M, Yang QZ, Wang GY, Chambon J, Wu YC, Fu KY, De Koninck Y, Zhang J. Dynamics of spinal microglia repopulation following an acute depletion. Sci Rep 2016;6:22839.
[72] Ydens E, Amann L, Asselbergh B, Scott CL, Martens L, Sichien D, Mossad O, Blank T, De Prijck S, Low D, Masuda T, Saeys Y, Timmerman V, Stumm R, Ginhoux F, Prinz M, Janssens S, Guilliams M. Profiling peripheral nerve macrophages reveals two macrophage subsets with distinct localization, transcriptome and response to injury. Nat Neurosci 2020;23:676–89.
[73] Zhao L, Zhang H, Liu X, Xue S, Chen D, Zou J, Jiang H. TGR5 deficiency activates antitumor immunity in non-small cell lung cancer via restraining M2 macrophage polarization. Acta Pharm Sin B 2022;12:787–800.
[74] Zhong S, Liu F, Giniatullin R, Jolkkonen J, Li Y, Zhou Z, Lin X, Liu C, Zhang X, Liu Z, Lv C, Guo Q, Zhao C. Blockade of CCR5 suppresses paclitaxel-induced peripheral neuropathic pain caused by increased deoxycholic acid. Cell Rep 2023;42:113386.
[75] Zuo G, Zhang T, Huang L, Araujo C, Peng J, Travis Z, Okada T, Ocak U, Zhang G, Tang J, Lu X, Zhang JH. Activation of TGR5 with INT-777 attenuates oxidative stress and neuronal apoptosis via cAMP/PKCε/ALDH2 pathway after subarachnoid hemorrhage in rats. Free Radic Biol Med 2019;143:441–53.